Fisheries and Oceans Canada | Pêches et Océans Canada
Ecosystems and Oceans Science | Sciences des écosystèmes et des océans

Canadian Science Advisory Secretariat (CSAS)

Research Document 2020/018

Newfoundland and Labrador Region

Physical Oceanographic Conditions on the Newfoundland and Labrador Shelf during 2018

F. Cyr, E. Colbourne, P.S. Galbraith, O. Gibb, S. Snook, C. Bishop, N. Chen, G. Han, D. Senciall

Science Branch
Fisheries and Oceans Canada
PO Box 5667
St. John's, NL A1C 5X1

April 2020

Canada

Foreword

This series documents the scientific basis for the evaluation of aquatic resources and ecosystems in Canada. As such, it addresses the issues of the day in the time frames required and the documents it contains are not intended as definitive statements on the subjects addressed but rather as progress reports on ongoing investigations.

Published by:

Fisheries and Oceans Canada
Canadian Science Advisory Secretariat
200 Kent Street
Ottawa ON K1A 0E6

http://www.dfo-mpo.gc.ca/csas-sccs/
csas-sccs@dfo-mpo.gc.ca

ISSN 1919-5044

Correct citation for this publication:

Cyr, F., Colbourne, E., Galbraith, P.S., Gibb, O., Snook, S., Bishop, C., Chen, N., Han, G., and D. Senciall. 2020. Physical Oceanographic Conditions on the Newfoundland and Labrador Shelf during 2018. DFO Can. Sci. Advis. Sec. Res. Doc. 2020/018 iv + 48 p.

Aussi disponible en français :

Cyr, F., Colbourne, E., Galbraith, P.S., Gibb, O., Snook, S., Bishop, C., Chen, N., Han, G., et D. Senciall. 2020. Conditions océanographiques physiques sur le plateau continental de Terre-Neuve et Labrador en 2018. DFO Can. Sci. Advis. Sec. Res. Doc. 2020/018 iv + 50 p.

TABLE OF CONTENTS

ABSTRACT

An overview of physical oceanographic conditions in the Newfoundland and Labrador (NL) Region during 2018 is presented as part of the Atlantic Zone Monitoring Program (AZMP). The winter North Atlantic Oscillation (NAO) index, a key indicator of the direction and intensity of the winter wind field patterns over the Northwest Atlantic was strongly positive during 2018. However, the spatial patterns of the associated atmospheric sea level pressure fields resulted in normal air temperatures, characterized by a warm month of March, a cold spring and a warm summer. The sea ice volume across the Newfoundland and Labrador Shelf, although close to the long-term mean, exhibited a strong negative anomaly in March as a consequence of warm air temperature over the Arctic during this month. Annual sea surface temperature (SST, based on infrared satellite imagery) trends on the Newfoundland and Labrador Shelf, while showing an increase of about 1°C since the early 1980s, were mostly below normal during 2018, e.g., up to -1.6 standard deviation (SD), and -1.9 SD for Hamilton Bank and Hudson Strait, respectively. In 2018, vertically averaged salinity at Station 27 was at its freshest (negative anomaly) since 1970. Observations from the summer AZMP oceanographic survey indicate that after a predominance of colder than average conditions since 2012, the volume of the cold intermediate layer (CIL, <0°C) reduced in 2018, especially in the northern part of the region where it was -1.6 SD below normal along the Seal Island section (second smallest volume since 1980). The spatially averaged bottom temperature during the spring in 3LNOPs remained slightly above normal at +1.0 SD in 2018. For the fall, bottom temperature in 2J3KLNO was also above normal at +0.8 SD, a return to positive anomaly after the cold anomaly of 2017 (the first one since 1995). The Labrador Current transport index along the Labrador and northern Newfoundland slope in 2018 was a record high since the beginning of the time series in 1993 (equal with 1994 at +1.7 SD) while it was lower than average on the Scotian slope. A new NL climate index was introduced. It was near normal in 2018, characterized by approximately an equal number of sub-indices above and below normal.

INTRODUCTION

This manuscript presents an overview of the 2018 environmental and physical oceanographic conditions in in the Newfoundland and Labrador (NL) Region (Figure 1). This report complements similar reviews of the environmental conditions in the Gulf of St. Lawrence and the Scotian Shelf and Gulf of Maine as part of the Atlantic Zone Monitoring Program (AZMP; Therriault et al. 1998; Galbraith et al. 2019; Hebert et al. in prep[1]). Physical oceanographic conditions for 2018 were presented in Cyr et al. 2019.

The information presented for 2018 is derived from various sources:

1. Observations made throughout the year at historical monitoring Station 27 near St. John's, NL;
2. Measurements made during the summer along standard AZMP cross-shelf sections (see Figure 1);
3. Oceanographic observations made during spring and fall multi-species resource assessment surveys;
4. Sea surface temperature (SST) data based on infrared satellite imagery of the Northwest Atlantic extracted using standard geographical boxes (see Figure 1);
5. Other multi-source historical data (ships of opportunity, international campaign, surveys from other Fisheries and Oceans Canada [DFO] regions, Argo program, etc.);
6. Ice data are from the Canadian Ice Service and meteorological data are from Environment Canada and other sources cited in the text.

Unless otherwise specified, the data are available from DFO's Marine Environmental Data Section (MEDS) archives and maintained in a regional data archive at the Northwest Atlantic Fisheries Centre (NAFC) in St. John's, NL.

Time series of temperature and salinity anomalies and other derived climate indices were constructed by removing the annual cycle computed over a standard climatological period from 1981 to 2010. Unless otherwise specified, annual or seasonal anomalies were normalized by dividing the values by the standard deviation (SD) of the data time series over the climatological period. A value of 2, for example, indicates that the index was 2 SD higher than its long-term average. As a general guide, anomalies within ±0.5 SD are considered to be normal.

The normalized values of water properties and derived climate indices are presented as "scorecards", which are color-coded gradations of 0.5 SD (Figure 2). Shades of blue represent cold-fresh environmental conditions and red represent warm-salty conditions. In some instances, such as NAO, or ice and cold water areas or volumes, negative anomalies may indicate warm conditions and are therefore colored red. Most of the colormaps used in this report are taken from the cmocean colormaps package for oceanography (Thyng et al. 2016).

[1] Hebert, D., Pettipas, R., and Brickman, D. In Prep. Meteorological, Sea Ice and Physical Oceanographic Conditions on the Scotian Shelf and in the Gulf of Maine during 2018. DFO Working Paper.

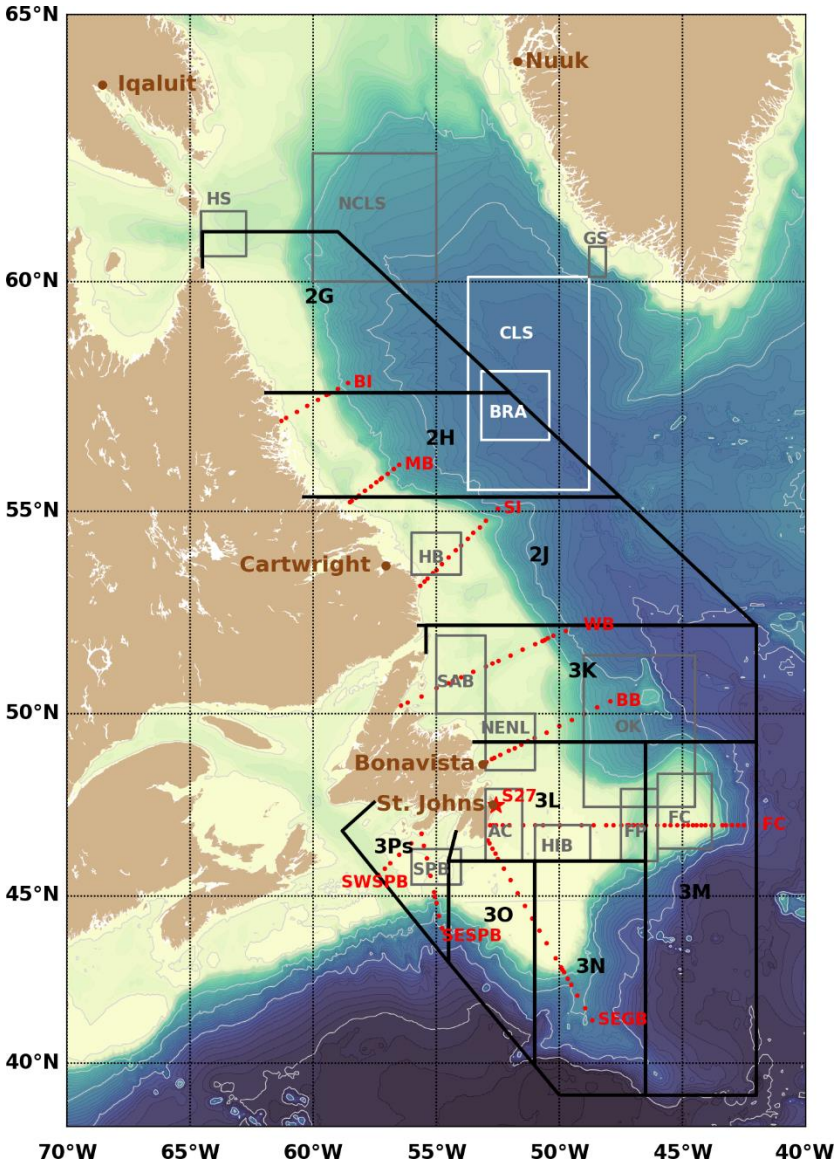

Figure 1. Map showing NAFO Divisions and main bathymetric features of the Northwest Atlantic. The hydrographic sections reported here are shown with red dots and the fixed Station 27 by a red star. The stations used for the air temperature time series are in brown. The standard boxes used to extract sea surface temperature anomalies are drawn in gray or white and listed here from north to south: Northern Central Labrador Shelf (NCLS), Hudson Strait (HS), Central Labrador Sea (CLS), Station Bravo (BRA), Hamilton Bank (HB), St. Anthony Basin (SAB), Northeast Newfoundland Shelf (NENL),Orphan Knoll (OK), Flemish Cap (FC), Flemish Pass (FP), Hibernia (HIB), Avalon Channel (AC) and Green-St. Pierre Bank (SPB).

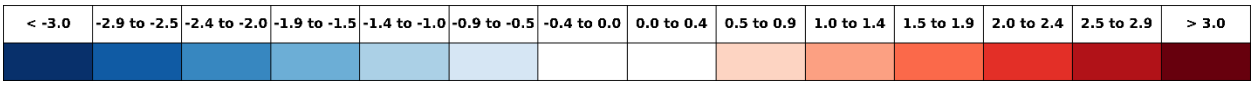

Figure 2. Colorscale used for the presentation of normalized anomalies. Color levels are incremented by 0.5 SD, where blue is below normal and red above normal. Values between 0 and ±0.5 SD remain white indicating normal conditions.

METEOROLOGICAL CONDITIONS

The North Atlantic Oscillation (NAO; see Figure 3 for time series since 1951 and Figure 4 for explicit values since 1980) refers to the anomaly in the sea-level pressure (SLP) difference between the sub-tropical high (average location near the Azores) and the subpolar low (average location near Iceland). Several definitions of the NAO exist and the one used here is from the National Center for Environmental Information of the National Oceanic and Atmospheric Administration (NOAA) available online. The winter NAO (defined here as the average of monthly values from December to February) is considered a measure of the strength of the winter westerly and north westerly winds over the Northwest Atlantic. A high NAO index (positive phase) occurs during an intensification of the Icelandic Low and Azores High. Except for some years for which the SLP patterns are spatially shifted (e.g., 1999, 2000 and 2018, where the location of high and low SLP were reversed in March), positive winter NAO years favor strong Northwest winds, cold air and sea surface temperatures, and heavy ice conditions on the NL shelves (Colbourne et al., 1994; Drinkwater 1996; Petrie et al., 2007). In 2018, the winter NAO was relatively high (1.3 SD above normal; first row in Figure 4), but the high-low pattern was reversed in March, which caused record-high temperatures above the Arctic (data not shown here). A predominance of strongly positive winter NAO phase has persisted since 2012, including the record high of +2.0 SD in 2015, whereas the record low of -3.1 SD was in 2010.

The Arctic Oscillation (AO) is a larger scale index intimately linked with the NAO. During a positive phase, the arctic air outflow to the Northwest Atlantic increases, resulting in colder winter air temperatures over much of the NL and adjacent shelf regions. Similarly to 2017, the AO was slightly above normal in 2018 (Figure 4) which is in contrast to 2015 when it was above normal at +1.5 SD (cold air temperatures) and to 2010 when it was below normal at -2.3 SD (warm air temperatures).

The Atlantic Multidecadal Oscillation (AMO), is also provided in Figure 4. This index, based on the SST of the Atlantic Ocean, evolves as part of a 65-80 year cycle that influences the regional climate and has consequences on the ocean circulation in the North Atlantic (e.g., Kerr 2000).

Air temperature anomalies (winter and annual values) from five coastal communities around the Northwest Atlantic (Nuuk Greenland, Iqaluit Baffin Island, Cartwright Labrador, Bonavista and St. John's Newfoundland; see Figure 1) are shown in Figure 4 as normalized anomalies between 1980 and 2018, and in Figure 5 and Figure 6 as cumulative annual and monthly anomalies, respectively. Except for Nuuk for which data are obtained from the Danish Meteorological Institute, the air temperature data from Canadian sites are from the second generation of Adjusted and Homogenized Canadian Climate Data (AHCCD) that accounts for shifts in station location and changes in observation methods (Vincent et al., 2012). On average, winter values in 2018 were normal for the three northern sites, but above normal for St. John's and Bonavista (+1.5 and +1.4 SD, respectively). The annual values were near normal at all stations except Bonavista (+0.8 SD). The predominance of warmer-than-normal air temperatures at all sites from the mid-1990s to 2013 is evident, where values in 2010 at Cartwright and Iqaluit reached 2.5 and 2.7 SD above normal setting 77 and 65 year records, respectively. The cumulative annual air temperature index was close to normal in 2018 in contrast to the lowest value since 1994 observed in 2015 (Figure 5). This decrease from 2017 however masks warmer-than-normal conditions at all stations in March, when Cartwright and Iqaluit were > 7°C above normal, followed by a colder than normal spring (May and June) at all stations (Figure 6). The NAO-related SLP pattern over the North Atlantic discussed above explains these intra-annual differences.

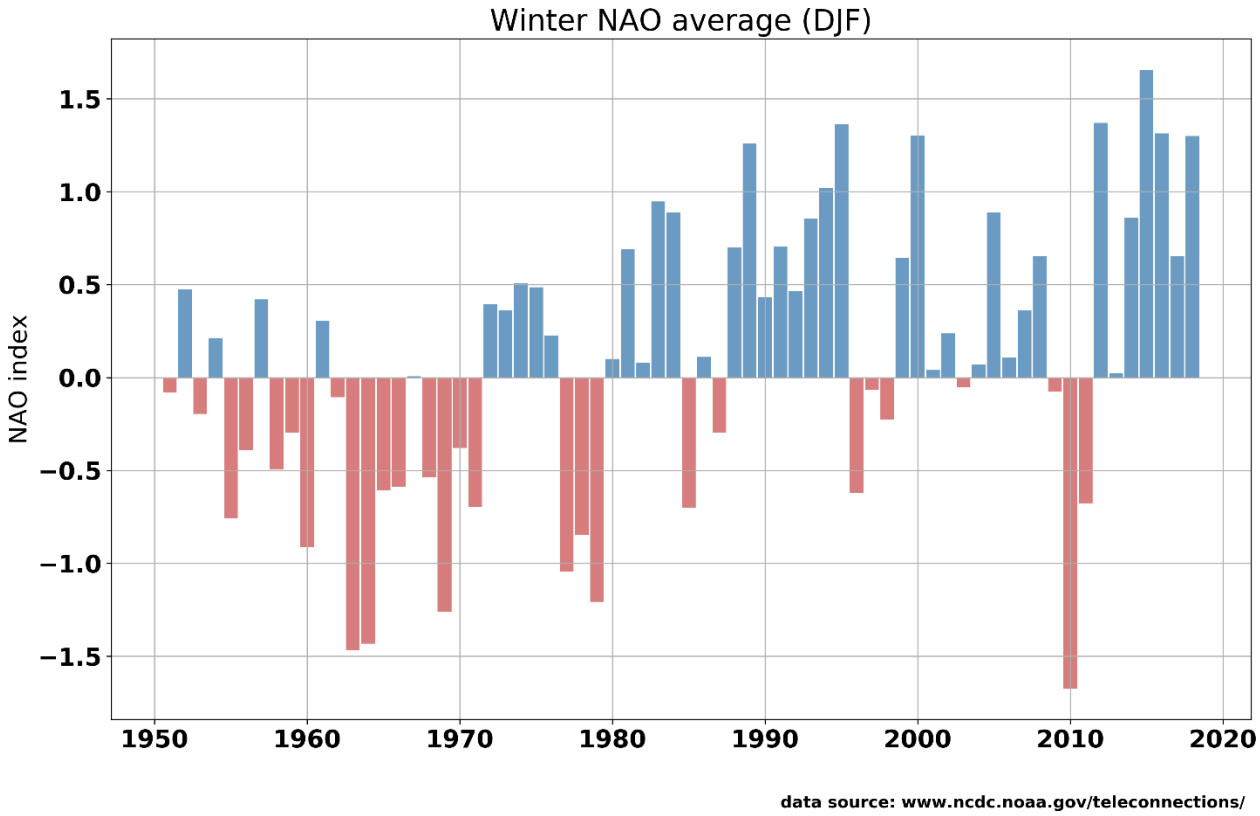

Figure 3. Winter North Atlantic Oscillation Index (NAO) calculated by averaging the December, January and February values since 1951 (which correspond to the average of December 1950 and January/February 1951). The NAO Index used here is from the National Center for Environmental Information of the NOAA. This index is used as part of the NL climate index mentioned in the summary (Figure 43).

	80	81	82	83	84	85	86	87	88	89	90	91	92	93	94	95	96	97	98	99	00	01	02	03	04	05	06	07	08	09	10	11	12	13	14	15	16	17	18	$\bar{x}$	sd
-- Climate indices --																																									
NAO_{winter}	-0.4	0.6	-0.4	0.9	0.9	-1.6	-0.3	-1.0	0.6	1.4	0.2	0.6	0.2	0.8	1.1	1.6	-1.5	-0.6	-0.9	0.5	1.5	-0.4	-0.1	-0.6	-0.4	0.9	-0.3	0.1	0.5	-0.6	-3.1	-1.5	1.6	-0.5	0.8	2.0	1.5	0.5	1.5		
AO	-1.4	-0.9	0.8	0.1	-0.4	-1.1	0.3	-1.2	0.2	2.3	2.4	0.5	1.1	0.3	1.3	-0.6	-1.0	0.0	-0.6	0.3	0.0	-0.3	0.2	0.4	-0.4	-0.8	0.4	0.7	0.5	-0.7	-2.3	1.3	-0.3	0.1	-0.1	1.5	-0.2	0.7	0.5		
AMO	-0.2	-0.5	-1.3	-0.5	-1.2	-1.6	-1.6	0.3	-0.1	-0.6	-0.3	-0.8	-1.3	-1.3	-1.1	0.6	-0.4	0.2	1.9	0.5	0.1	0.5	0.3	1.2	1.0	1.5	1.4	0.7	0.7	0.1	1.8	0.5	1.1	0.8	0.5	0.5	1.8	1.6	0.3		
-- Winter Air Temperature --																																									
StJohns	-0.3	0.9	0.0	0.8	0.6	-0.6	-0.1	-0.9	0.0	-1.4	-2.1	-1.1	-1.6	-1.5	-1.2	-0.8	0.4	0.2	0.3	1.3	1.5	-0.6	0.3	-0.6	1.0	0.7	1.7	0.3	0.0	1.1	1.3	2.5	1.2	0.7	-0.7	0.7	1.0	0.3	1.5	-3.7	1.2
Bonavista	0.2	0.9	0.0	0.1	0.0	-0.7	-0.1	-0.5	0.2	-1.1	-2.0	-1.1	-1.5	-1.9	-1.5	-0.6	0.8	0.1	0.5	1.1	1.3	0.0	0.6	-0.6	1.2	0.7	1.8	0.3	-0.2	0.7	1.4	2.3	1.0	0.9	-1.0	0.4	1.0	0.3	1.4	-3.5	1.3
Cartwright	0.5	1.0	0.3	-1.2	-0.9	-0.1	0.2	-0.1	0.1	-1.2	-1.2	-1.3	-1.5	-1.4	-1.0	-0.7	0.7	0.3	0.8	0.5	0.3	0.0	0.4	0.3	1.8	0.0	0.7	0.9	-0.8	0.2	2.9	2.2	0.1	0.9	-0.7	-1.2	0.4	-0.1	0.3	-12.3	2.5
Iqaluit	0.6	0.9	1.0	-1.8	-1.6	0.8	1.7	-0.9	-0.1	-1.3	-0.8	-1.3	-0.6	-1.7	-0.5	0.1	0.4	0.3	-0.4	0.1	0.4	0.5	0.1	0.5	0.9	-0.3	0.6	1.3	-0.7	0.2	2.3	2.2	0.8	0.8	0.7	-0.8	0.3	0.5	0.3	-25.0	3.4
Nuuk	0.7	0.3	0.3	-2.0	-2.5	0.5	1.8	-0.2	0.4	-0.8	-0.3	-0.6	-0.9	-1.7	-0.4	-0.8	0.5	0.2	0.1	-0.1	0.2	0.6	0.2	0.9	1.1	0.3	0.6	0.9	-1.0	0.6	1.9	1.2	0.2	0.6	0.2	-0.6	0.1	0.2	-0.3	-7.7	3.0
-- Annual Air Temperature --																																									
StJohns	-1.2	1.0	-1.0	0.5	0.2	-1.7	-1.0	-0.5	0.2	-0.6	-0.5	-1.4	-1.7	-1.5	-0.5	-0.7	0.3	-1.1	0.6	1.9	1.0	0.3	-0.4	0.4	0.6	0.7	1.6	-0.1	0.8	0.9	1.7	0.6	2.3	0.8	0.4	-0.7	0.7	0.4	0.4	5.0	0.8
Bonavista	-1.0	0.7	-1.0	0.1	-0.4	-1.4	-0.9	-0.2	0.2	-0.2	-0.6	-1.8	-1.8	-1.8	-0.7	-0.7	0.6	-0.9	0.6	1.5	0.8	0.6	-0.1	0.5	1.0	1.2	1.7	0.0	0.7	0.5	1.6	0.8	1.7	1.1	0.5	-0.5	0.6	0.1	0.8	4.7	0.9
Cartwright	-0.1	1.1	-1.3	-0.5	-1.1	-0.6	-0.9	0.5	-0.3	-0.6	-1.3	-1.6	-1.4	-1.3	-0.6	-0.3	0.5	-0.3	0.6	1.1	0.5	0.6	-0.3	0.4	1.1	0.9	1.8	0.1	0.1	0.4	2.5	0.7	1.4	0.5	0.0	-1.2	-0.3	0.2	-0.2	0.1	1.3
Iqaluit	0.6	1.3	-0.8	-1.5	-1.1	1.1	-0.7	-0.7	-0.1	-1.1	-1.2	-0.5	-1.7	-1.7	-0.4	0.5	0.5	0.3	0.2	0.1	0.4	0.6	-0.1	0.8	0.1	0.9	1.4	0.2	-0.1	0.5	2.7	0.5	0.6	0.2	0.4	-1.2	0.4	0.7	-0.2	-9.1	1.8
Nuuk	0.6	0.1	-1.0	-1.8	-2.0	1.2	0.1	0.0	0.3	-1.2	-0.7	-0.4	-1.4	-1.6	-0.6	-0.2	0.4	0.1	0.2	-0.2	0.4	0.8	0.2	1.3	0.6	1.1	0.7	0.5	0.2	0.5	2.6	-0.2	0.9	0.6	0.5	-1.0	1.3	0.4	-0.2	-1.4	1.5

Figure 4. Scorecard of normalized large-scale indices (winter NAO, AO and AMO) and air temperature anomalies (winter and annual) for five cities between 1980 and 2018. Mean and standard deviation for the air temperatures during the 1981-2010 period are provided in the last column (in °C). No mean or standard deviation is provided for the large-scale indices (grayed boxes).

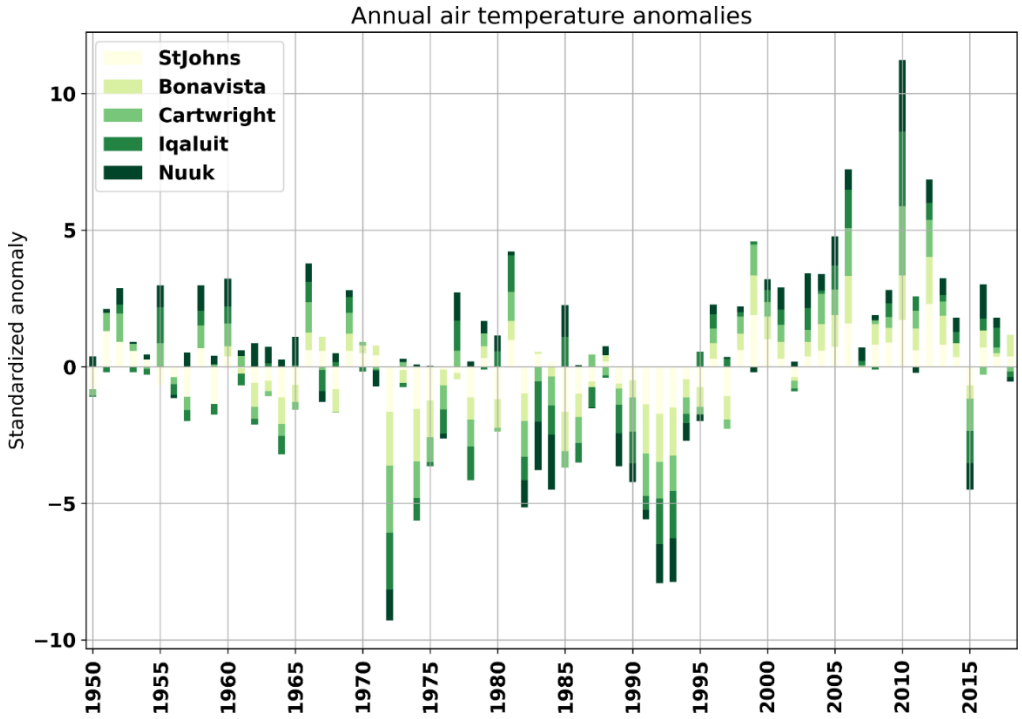

Figure 5. Cumulative normalized annual air temperature anomalies time series at Nuuk, Iqaluit, Cartwright, Bonavista and St. John's. The average of these five time series is used to construct the NL climate index mentioned in the summary (Figure 43).

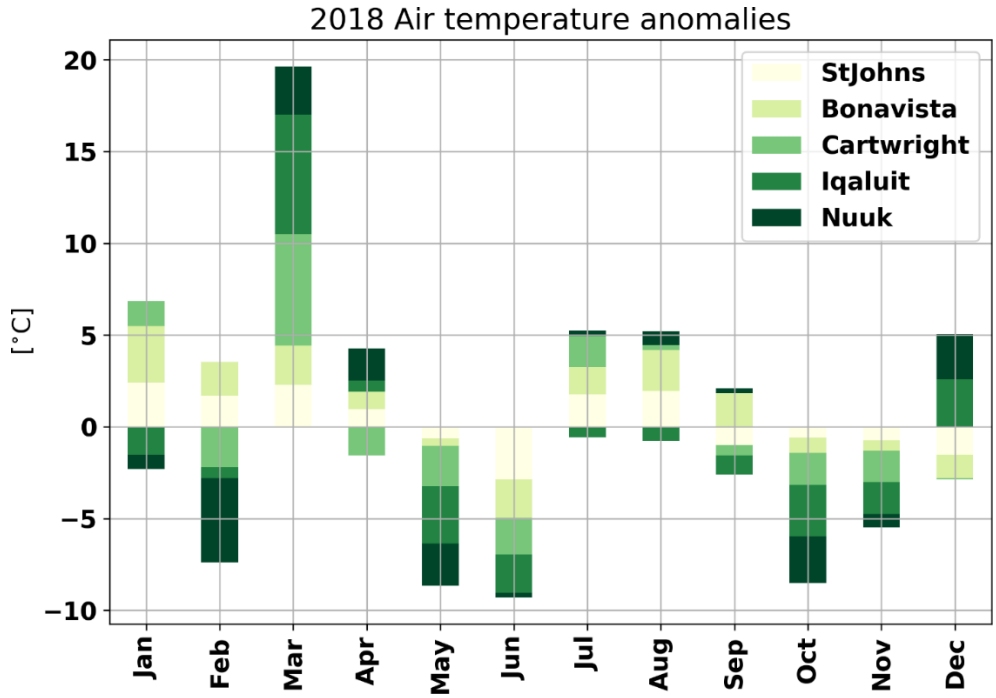

Figure 6. Cumulative monthly air temperature anomalies at Nuuk, Iqaluit; Cartwright, Bonavista and St. John's, NL for 2018.

SEA ICE CONDITIONS

Ice cover area, volume and seasonal duration are estimated from ice cover products obtained from the Canadian Ice Service (CIS). These parameters consist of weekly Geographic Information System (GIS) charts covering the period 1969-2018 and daily charts covering the period 2009-2018. All charts were further processed into regular 0.01° latitude by 0.015° longitude grids (approximately 1 km resolution), with ice concentrations and growth stages attributed to each grid point. Average thicknesses (and therefore regional volumes) are estimated from standard thicknesses attributed to each stage of ice growth from new ice and nilas (5 cm), grey ice (12.5 cm), grey-white ice (22.5 cm), thin first year ice (50 cm), medium first year ice (95 cm) and thick first year ice (160 cm). Prior to 1983, the CIS reported ice categories with fewer classifications, where a single category of first year ice (≥30 cm) was used with a suggested average thickness of 65 cm. We have found this value to lead to underestimates of the seasonal maximum thickness and volume based on high interannual correlations between the estimated volume of the weekly seasonal maximums and its area or sea-ice season duration. The comparisons of these correlations pre- and post-1983 provided estimates of first-year ice thickness of 85 cm in the Gulf of St. Lawrence and 95 cm on the Newfoundland and Labrador Shelf for this single first year ice category, which were used instead of the suggested 65 cm.

Several products were computed to describe the sea-ice cover inter-annual variability. The day of first and last occurrence duration (Figure 7) and distribution of ice thickness during the week of maximum volume (Figure 8) are presented as maps. Regional scorecards of anomalies in the first and last day of ice, duration of the sea ice season and maximum ice volume are presented in Figure 9 for the Labrador and Newfoundland shelves. Here, the area defined as Labrador shelf spans from 52°15'N to 55°20'N, matching the latitude limits of NAFO Division 2J, and the area defined as the Newfoundland Shelf is to the south. Daily evolution of the ice volume during the 2018 ice season is presented in Figure 10 for Labrador (left) and Newfoundland (right) shelves in relation to the climatology and historical extremes. Time series of seasonal maximum ice volume, area (excluding thin new ice) and ice season duration in relation to the December-to-April air temperature anomaly at Cartwright are presented for Labrador (top) and Newfoundland (bottom) shelves in Figure 11.

Ice typically starts forming in December along the Labrador coast and only by late February at the southern extent of sea-ice presence (Figure 7). Last occurrence is typically in late June to early July on the Labrador coast, leading to sea-ice season durations of 23 weeks or more. There has been a declining trend in ice cover severity since the early 1990s reaching the lowest values in 2011 and 2010, with a rebound in 2014 (Figure 9 and Figure 11). The sea ice metrics of annual maximum ice volume and annual maximum area ice cover duration are well correlated with each other (r^2 = 0.77; Figure 11). The best correlation with air temperature was between the December-April air temperature anomaly at Cartwright and the sea-ice metrics of the Newfoundland Shelf (r^2 = 0.70-0.81), indicative of the advective nature of the Newfoundland Shelf sea ice; i.e., strong ice cover is associated with cold air temperatures in the source area. Sensitivity of the Newfoundland Shelf ice cover to air temperature increase (e.g. through climate change) can thus be estimated using 1969-2018 co-variations between winter air temperature and sea-ice parameters, which indicate losses of 16 km^3, 26,000 km^2 and 17 days of sea-ice season for each 1°C increase in winter air temperature. These values are similar to those obtained for the Gulf of St. Lawrence (Galbraith et al., 2019). An overview of sea ice conditions (volume and season duration) for NL since 1969 is presented in Figure 12. It suggests that 2018 was just below normal, in contrast with the low ice conditions of the early 2010s.

In 2018, the sea-ice cover first appeared at a date ranging from near-normal to later than normal by a few weeks (Figure 7), leading to regional averages that were earlier-than normal on the

Labrador Shelf and near-normal on the Newfoundland Shelf (Figure 9). Last occurrence varied between later than normal near-shore to earlier than normal offshore (Figure 7), averaging to near-normal timing (Figure 9). Sea ice volume progressed below normal until April on the Labrador Shelf, and up to late February on the Newfoundland Shelf (Figure 10). The ice cover declined sharply on the Newfoundland Shelf in March before rebounding to near-normal conditions for the time of year by late April. The seasonal maximum combined ice volume was below normal at 94 km^3 (-0.8 SD) during the week of April 16th (Figure 8) which is a bit late. The durations of 170 and 113 days on the Labrador and Newfoundland Shelves respectively were near-normal (-1.1 SD).

Iceberg counts obtained from the International Ice Patrol of the US Coast Guard indicate that 208 (-0.9 SD) icebergs drifted south of 48°N onto the Northern Grand Bank during 2018, down from 1,008 in 2017 (Figure 13). There were only 1 in 2010, 2 in 2011, 13 in 2013 and 499 in 2012. The 119-year average is 489 and the 1981-2010 average is 767. In some years during the cold periods of the early 1980s and 1990s, over 1,500 icebergs were observed south of 48°N with an all-time record of 2,202 in 1984. Only 2 years (1966 and 2006) in the 118-year time series reported no icebergs south of 48°N. Years with low iceberg numbers on the Grand Banks generally correspond to higher than normal air temperatures, lighter than normal sea-ice conditions, and warmer than normal ocean temperatures on the NL Shelf. Monthly iceberg numbers during 2018 show below normal counts for all months relative to the 1981-2010 average (Figure 14).

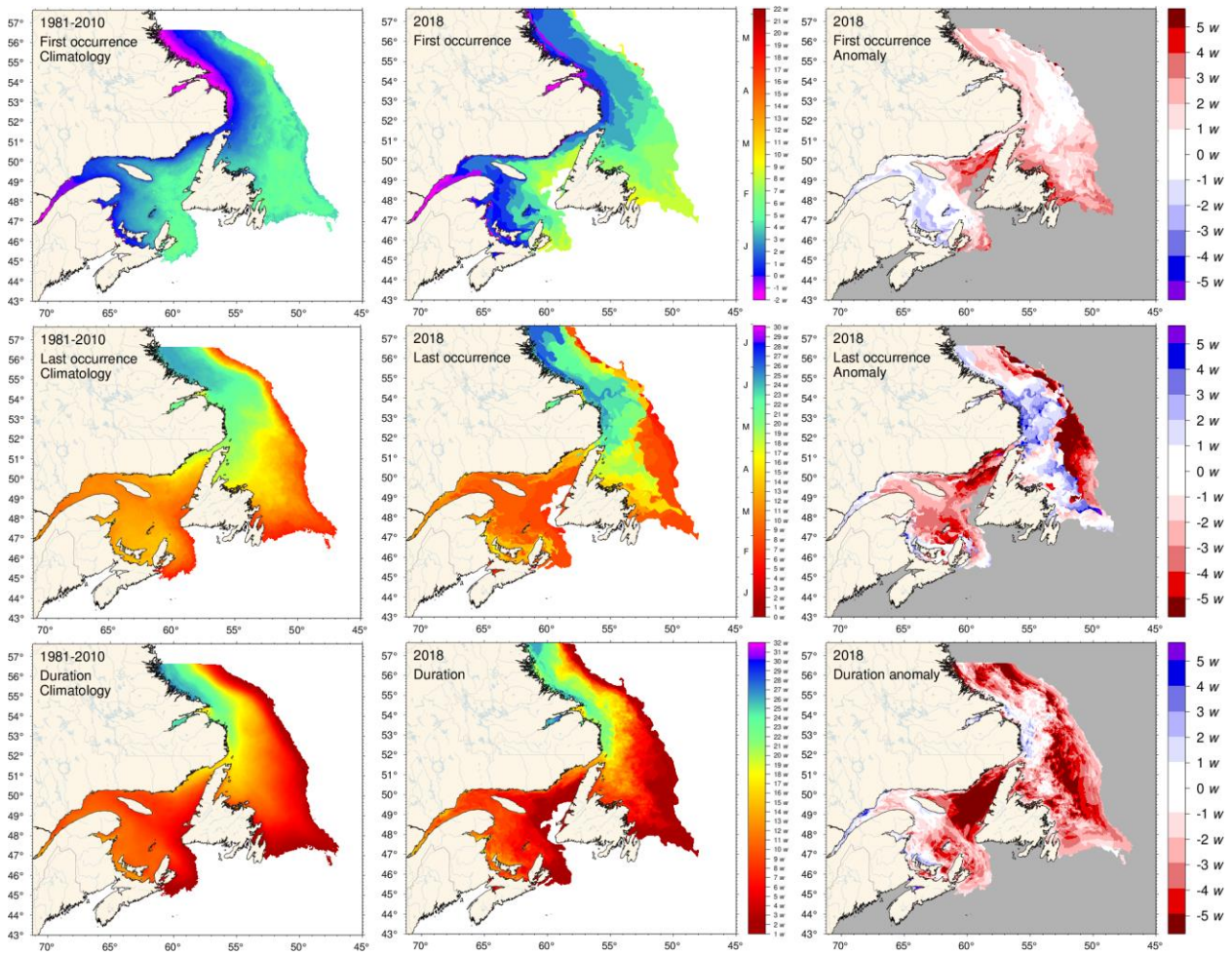

Figure 7. First (top) and last (middle) occurrence of ice and ice season duration (bottom) based on weekly data. The 1981-2010 climatologies are shown (left) as well as the 2018 values (middle) and anomalies (right). First and last occurrence is defined here as the first and last weekly chart in which any amount of ice is recorded for each pixel and are illustrated as day-of-year. Ice duration sums the number of weeks with ice cover for each pixel. Climatologies are shown for pixels that had at least 15 years out of 30 with occurrence of sea-ice, and therefore also show the area with 50% likelihood of having some sea-ice at any time during any given year. The duration anomaly map includes pixels with no ice cover where some was expected based on the climatology.

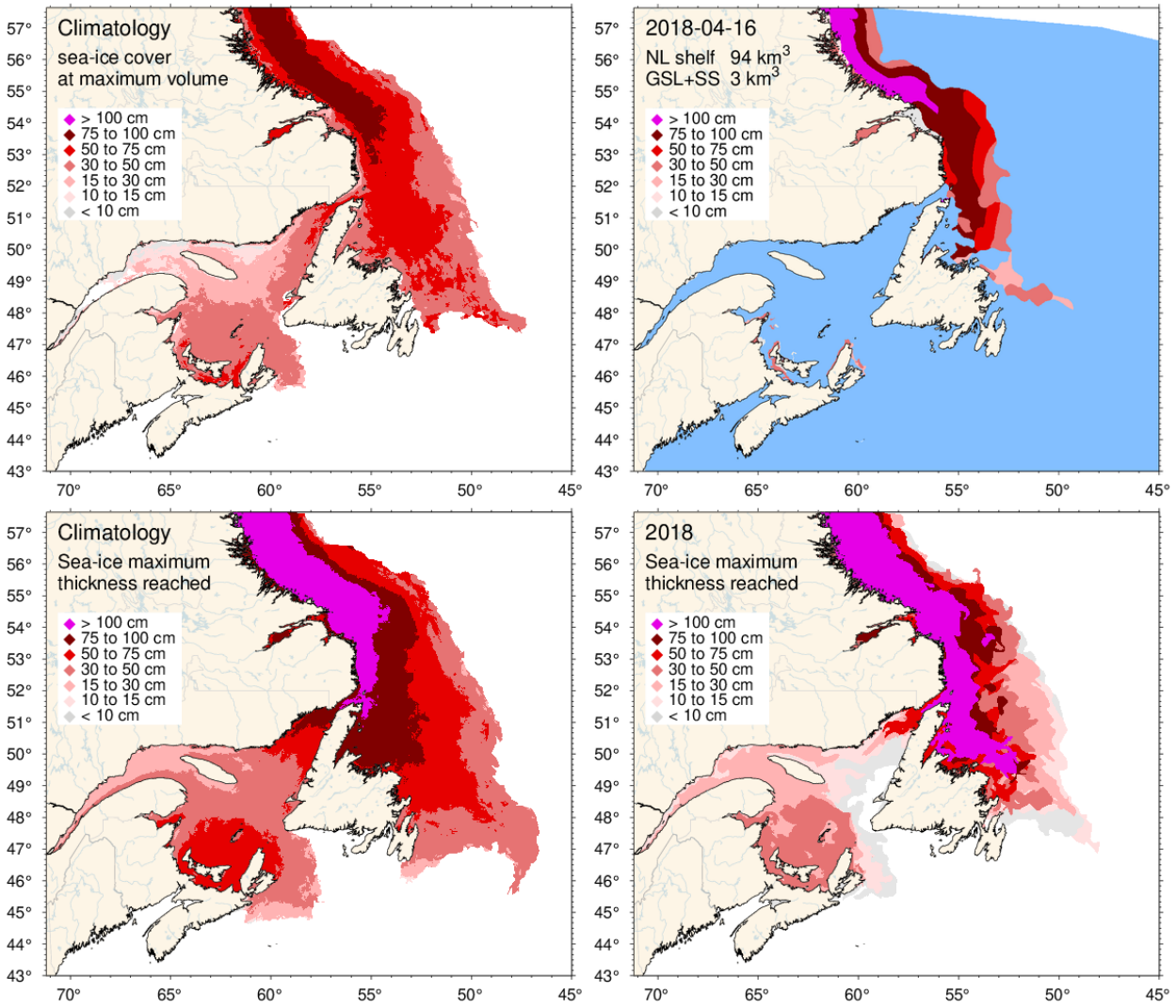

Figure 8. Ice thickness map for 2018 for the week with the maximum annual volume on the Newfoundland and Labrador Shelf (upper right panel) and similarly for the 1981-2010 climatology of the weekly maximum (upper left panel). Note that these maps reflect the ice thickness distribution on that week. The maximum ice thickness observed at any given location during the year is presented in the lower panels, showing the 1981-2010 climatology and 2018 distribution of the thickest ice recorded during the season at any location.

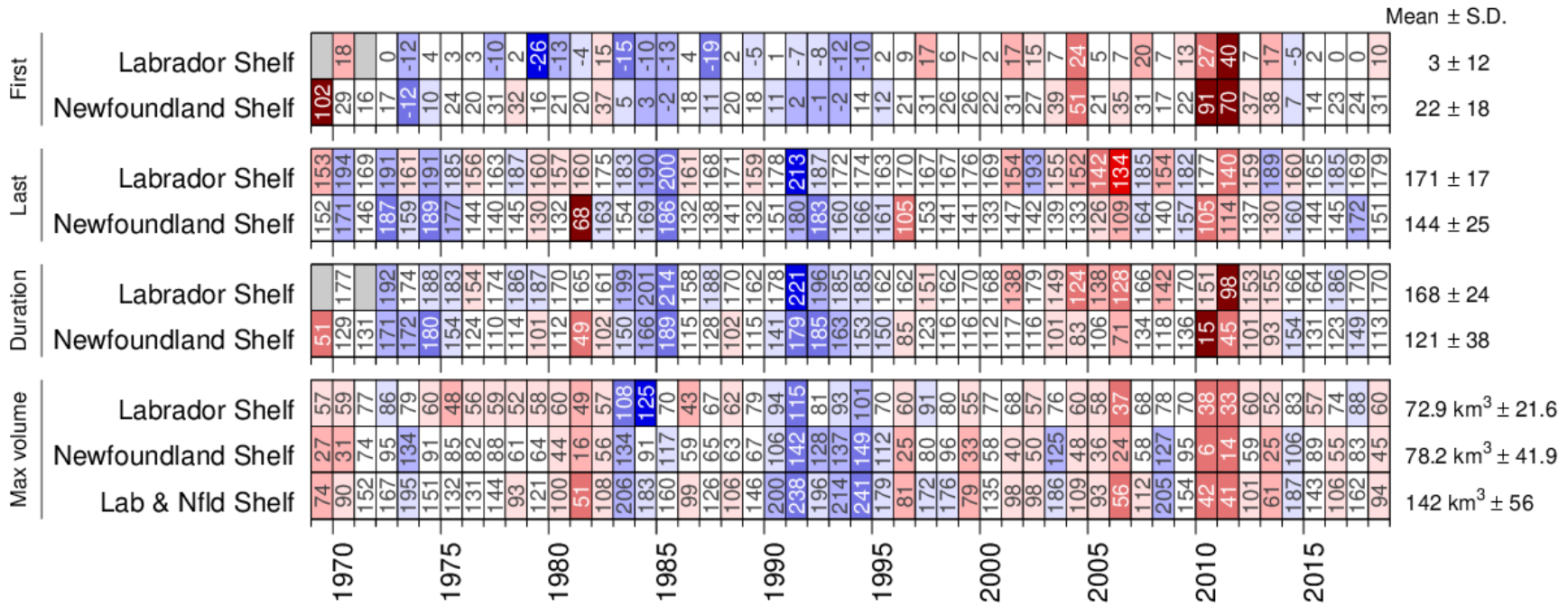

Figure 9. First and last day of ice occurrence, ice duration, and maximum seasonal ice volume by region. The moment when ice was first and last observed in days from the beginning of each year is indicated for each region, and the color code expresses the anomaly based on the 1981–2010 climatology, with blue (cold) representing earlier first occurrence and later last occurrence. The threshold is 5% of the climatological average of the seasonal maximum ice volume. Numbers in the table are the actual day of the year or volume, but the color coding is according to normalized anomalies based on the climatology of each region. Duration is the numbers of days that the threshold was exceeded.

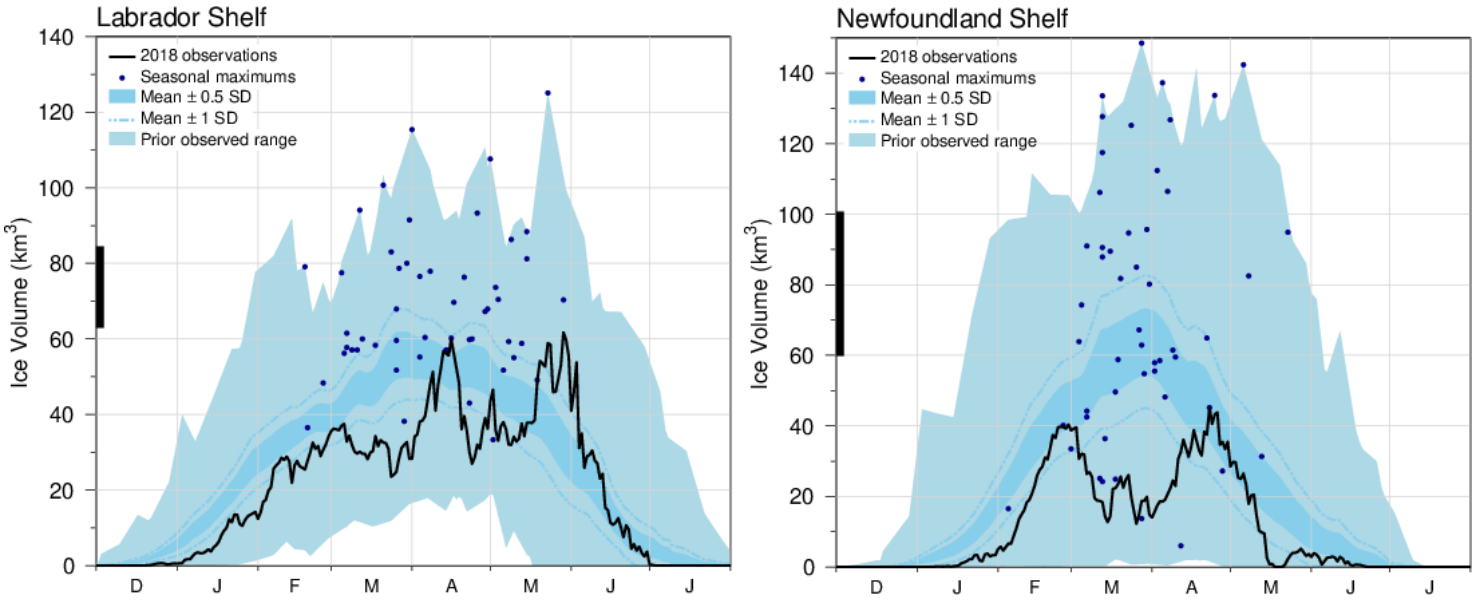

Figure 10. Time series of the 2017-2018 daily mean ice volume (black lines) for the Labrador Shelf (left) and Newfoundland Shelf (right), the 1981-2010 climatological mean volume ±0.5 and ±1 SD (dark blue area and dashed line respectively), the minimum and maximum span of 1969-2018 observations (light blue), and the date and volumes of 1969-2018 seasonal maximums (blue dots). The black thick line on the left indicates the mean volume ±0.5 SD of the annual maximum ice volume, which is higher than the peak of the mean daily ice volume distribution.

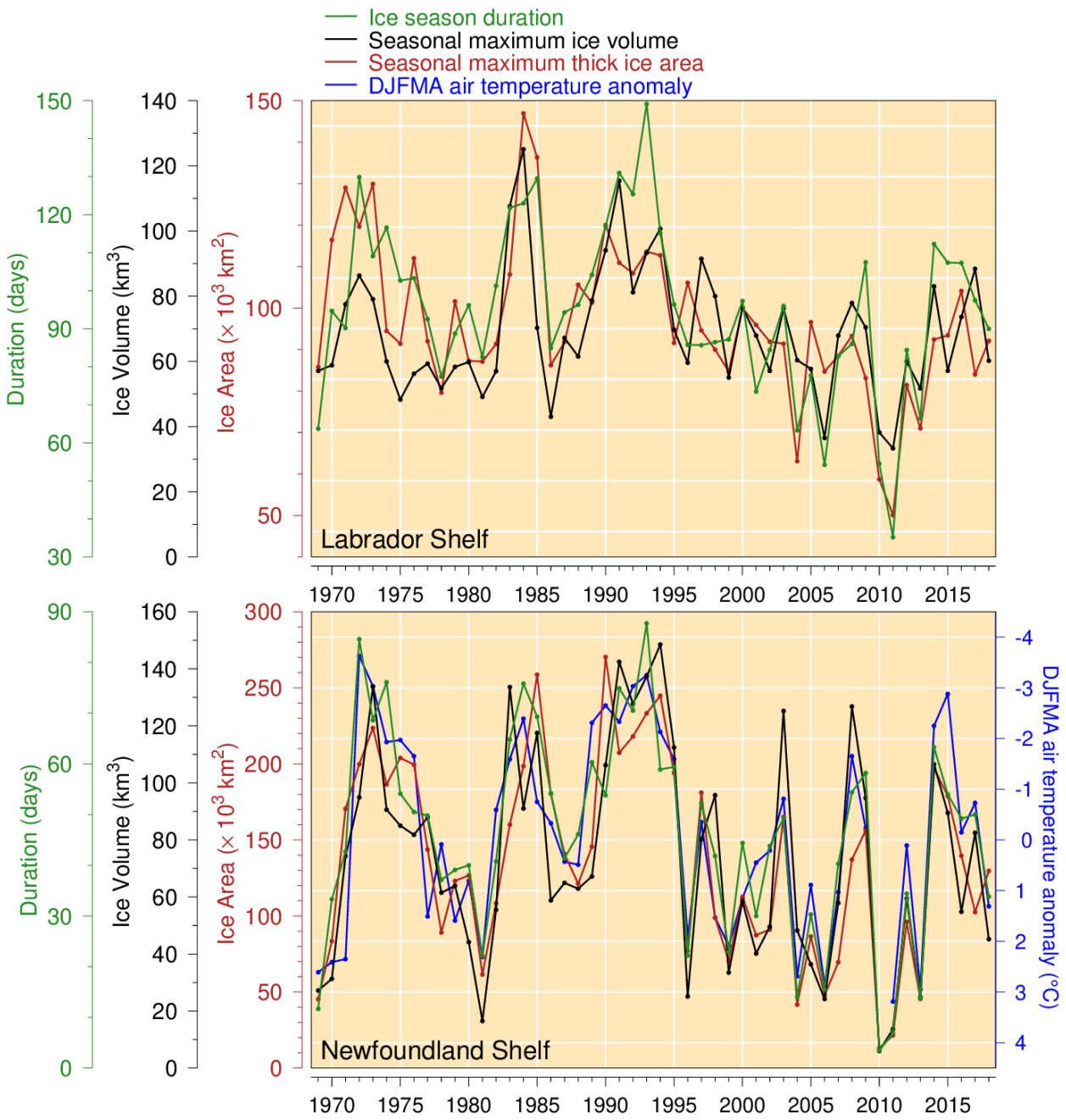

Figure 11. Seasonal maximum ice volume and area (excluding ice less than 15 cm thick), and ice season duration for the Labrador Shelf (top) and Newfoundland Shelf (bottom), and December-to-April air temperature anomaly at Cartwright.

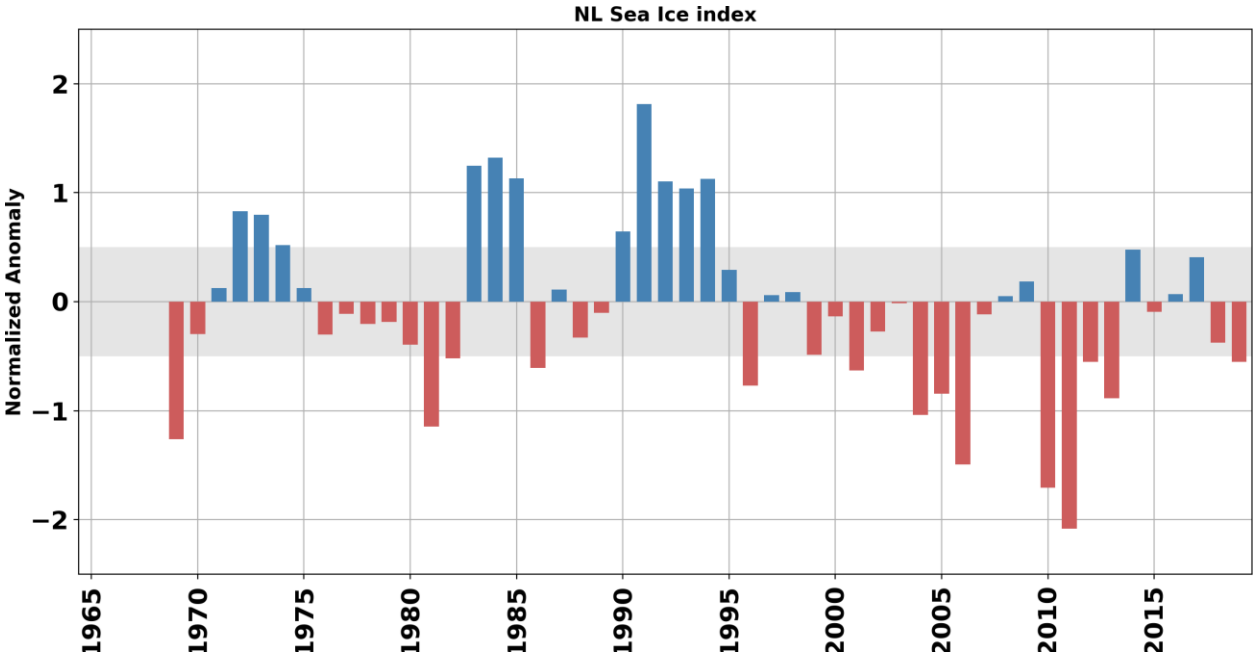

Figure 12. Newfoundland and Labrador sea ice index established by averaging the normalized anomalies of volume and duration of sea ice for Newfoundland and Labrador shelves (black and green time series in Figure 11). Shaded gray areas represent the ±0.5 SD range considered "normal". This sea ice index contributes to the NL climate index described in the summary (Figure 43).

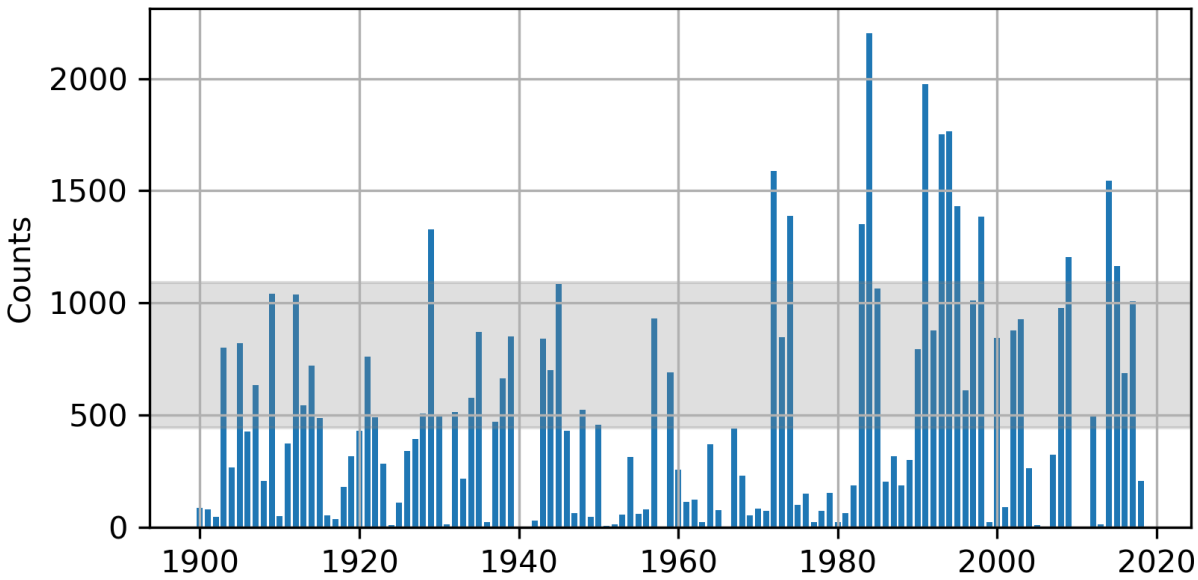

Figure 13. Annual iceberg count crossing south of 48°N on the northern Grand Bank. The shaded area corresponds to the 1981-2010 average ±0.5 SD. Data courtesy of IIP of the USCG. The normalized anomaly of this time series contributes to the NL climate index described in the summary (Figure 43).

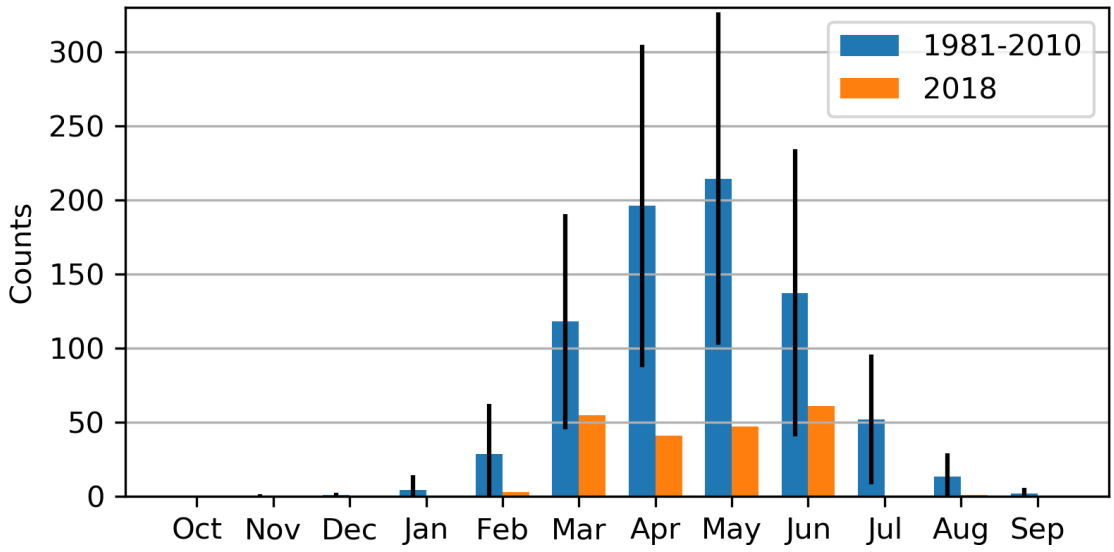

Figure 14. Monthly iceberg count crossing south of 48°N on the northern Grand Bank during the annual iceberg season (from October to September). The vertical bars on the 1981-2010 average correspond to ±0.5 SD. Data courtesy of IIP of the USCG.

SATELLITE SEA-SURFACE TEMPERATURE CONDITIONS

The 4 km resolution Pathfinder 5.2 sea surface temperature (SST) database (Casey et al., 2010) was used to provide annual estimates of the SST within 14 sub-areas in the Northwest Atlantic (see Figure 1). We used this data set from 1981 to 2010 and in more recent years (2011-2018) we use data from NOAA and EUMETSAT satellite data provided by the remote sensing group in the Marine Ecosystem Section at the Bedford Institute of Oceanography (BIO).

A least squares fit of the Pathfinder and NOAA temperatures during the period 1997-2012 is given by SST (Pathfinder) = 0.989*SST (NOAA) -0.02 with an r^2 = 0.98 (Hebert et al., 2012). The recent NOAA SST data were then adjusted accordingly and anomalies computed based on 1981-2010 averages. A comparison of the Pathfinder data with near-surface measurements indicate that SST derived from night satellite passes provided the best fit with in situ data. Data were not available for every month in some of the northern areas due to sea ice cover.

The 2018 monthly SST anomalies for the 14 sub-areas mentioned above are presented in Figure 15 and show that SST were generally colder than normal between April and July and warmer than normal between August and October, except for Labrador. In November, while most of the regions exhibited colder than normal conditions, SST for the Greenland Shelf box (easternmost region) was 2.0 SD above average.

Figure 16 shows scorecards of annual anomalies for these regions. This figure exhibits colder than normal conditions for all regions between 1981 and 1993, followed by warmer than normal conditions that lasted until approximately 2014. Recent years consist of slightly colder than normal conditions, including those for 2018 that were especially cold along the Labrador coast, e.g., -1.9, -1.6 and -0.9 SD below normal for Hudson Strait, Hamilton Bank and St. Anthony Basin, respectively. The annual time series of the average SST anomalies over all these regions is presented in Figure 17 as a bar graph. On average for all 14 regions, the SST was 0.6 SD below normal, in accordance with the near decadal pattern observed in the winter NAO index, for example.

	-- 2018 Monthly Sea Surface Temperature anomalies --											
	J	F	M	A	M	J	J	A	S	O	N	D
Greenland Shelf (GS)	-0.7	-0.6	-0.6	-0.2	-0.3	-0.3	-1.1	1.3	1.1	0.9	2.0	0.6
NC Lab. Sea (NCLS)	0.1	0.0	-0.1	-0.3	-1.2	-1.3	-0.9	-0.1	-0.1	-0.2	-0.6	0.3
Hudson Strait (HS)	-0.5		-0.5	-0.4	-1.2	-2.2	-2.0	-0.8	-0.7	-0.2	-1.8	-0.8
Cent. Lab. Sea (CLS)	-0.2	0.0	0.1	0.0	-0.5	-0.2	-0.7	-0.2	-0.5	-0.7	-0.8	-0.8
Bravo (BRA)	0.0	-0.4	0.6	0.2	-0.5	0.1	-0.6	-0.1	-0.5	-0.8	-0.5	-1.3
Hamilton Bank (HB)	-0.6	-0.6	-0.7	-0.9	-0.8	-1.5	-0.5	-0.6	-2.0	-0.9	-0.1	-0.9
St. Anthony B. (SAB)	-1.0	-0.8	-0.7	-1.6	-0.8	-1.7	-0.2	0.2	-0.4	-0.5	0.2	0.8
NE NF shelf (NENL)	0.0	-0.6	-0.7	-1.6	-1.0	-2.1	-0.7	1.1	0.5	-0.3	-0.5	0.1
Orphan Knoll (OK)	0.0	-0.2	0.6	0.0	-0.7	-1.5	-1.4	0.2	0.8	0.6	-0.9	-0.2
Avalon Channel (AC)	0.9	1.0	0.6	-0.6	-0.3	-1.8	-2.2	1.0	1.1	0.6	-1.1	-0.6
Hibernia (HIB)	0.9	1.2	0.9	-0.1	0.0	-0.9	-2.0	0.8	1.3	0.4	-0.7	-1.1
Flemish Pass (FP)	-0.4	-0.7	-0.1	-0.6	-1.1	-1.5	-1.8	0.9	1.2	0.7	-1.4	-0.1
Flemish Cap (FC)	-0.6	-0.1	-0.1	-0.8	-1.4	-1.4	-1.8	0.6	1.2	1.2	-1.6	-1.1
St.Pierre Bank (SPB)	0.0	1.6	0.7	-0.1	-0.2	-1.5	-1.7	1.0	1.7	1.0	-0.9	-1.0

Figure 15. Normalized monthly anomalies of 2018 SST for NL regions (see boxes Figure 1)

	-- Sea Surface temperature anomalies --																																						
	81	82	83	84	85	86	87	88	89	90	91	92	93	94	95	96	97	98	99	00	01	02	03	04	05	06	07	08	09	10	11	12	13	14	15	16	17	18	$\bar{x}$	sd
Greenland Shelf (GS)	-1.6	-1.5	-1.8	-1.2	0.7	-0.1	0.3	-0.3	-1.6	-0.8	0.3	-0.7	-0.2	0.3	1.9	0.0	0.6	-0.2	-0.9	-0.3	0.1	0.5	1.8	1.0	1.0	0.0	0.1	-0.1	0.7	2.0	-0.3	0.4	0.4	0.5	-0.3	1.1	0.3	0.2	1.5	0.9
NC Lab. Sea (NCLS)	-1.4	-1.1	-1.4	-1.4	-0.3	0.4	-0.8	-0.1	-1.1	-1.1	-0.4	-0.5	-0.9	-0.4	-0.4	0.4	0.7	0.8	-0.5	-0.3	0.9	0.8	1.4	1.6	1.5	1.2	0.7	-0.3	-0.3	2.2	0.0	-0.2	0.0	-0.1	-0.7	0.4	-0.1	-0.4	2.8	1.1
Hudson Strait (HS)	-1.5	-0.1	-0.3	-1.1	-0.3	1.3	0.6	-0.6	-1.2	0.8	0.5	0.6	1.1	1.2	2.8	0.2	-0.7	-0.8	-1.9	-0.2	-0.2	0.0	-0.2	0.2	0.5	-0.4	-1.1	-0.8	-0.2	1.7	-0.8	0.0	-1.3	-0.6	-1.3	-0.5	-1.6	-1.9	0.1	0.4
Cent. Lab. Sea (CLS)	-0.9	-1.4	-1.7	-2.0	-0.9	-0.5	-0.2	-0.2	-0.8	-1.1	-0.3	-0.4	-0.9	-0.1	-0.6	0.0	0.8	0.7	0.0	-0.2	0.7	0.3	1.5	1.2	1.3	1.5	1.0	1.1	0.3	1.8	0.3	0.8	0.6	0.8	-0.1	0.5	0.3	-0.4	4.2	0.9
Bravo (BRA)	-1.3	-1.1	-2.0	-1.6	-1.1	-0.8	-0.4	-0.4	-0.7	-1.1	-0.4	-0.5	-0.4	-0.3	0.0	0.0	0.8	0.6	0.1	-0.2	0.5	0.2	1.5	1.1	1.4	1.6	1.0	1.3	0.3	1.7	0.4	1.1	0.5	1.0	0.0	0.5	0.3	-0.4	4.3	0.8
Hamilton Bank (HB)	-1.7	-0.6	-0.5	-1.0	-0.9	-0.5	-0.5	-0.5	-0.1	0.0	-1.1	-1.1	0.4	1.1	2.6	-1.5	-0.2	0.5	-0.5	0.7	0.0	-0.9	0.9	0.8	0.9	1.5	-0.5	1.6	-0.3	1.1	0.7	1.6	-0.6	0.3	-0.3	-0.6	-0.1	-1.6	1.5	0.5
St. Anthony B. (SAB)	-1.9	-0.8	-0.4	-0.8	-0.5	-0.6	-0.5	-0.2	0.8	-0.8	-1.1	-1.1	-0.8	1.5	-0.5	-0.8	-0.1	0.7	0.3	0.8	0.2	-0.7	0.7	1.1	1.7	2.3	-0.7	1.5	-0.5	1.1	0.6	1.7	-0.3	0.6	-0.8	-0.5	-0.3	-0.9	2.6	0.6
NE NF shelf (NENL)	-2.3	-0.6	-0.2	-0.5	-0.9	-0.6	-0.2	0.0	-0.1	0.2	-1.7	-1.4	-0.7	1.3	1.9	-0.5	-0.7	0.7	0.4	0.5	0.2	-0.5	0.3	0.9	1.5	1.9	-0.4	1.2	-0.5	0.8	0.5	1.1	0.3	0.8	-0.8	-0.4	-0.3	-0.5	3.5	0.7
Orphan Knoll (OK)	-1.3	-0.6	-0.3	-1.4	-2.0	-0.5	0.1	0.3	-0.9	-0.8	-1.4	-1.1	-0.9	-0.9	0.2	0.1	0.4	0.8	0.5	0.5	0.6	0.0	0.5	1.3	1.9	1.9	0.7	1.2	-0.1	1.3	0.8	1.7	0.8	0.6	-0.9	0.0	0.4	-0.3	6.0	0.8
Avalon Channel (AC)	-1.8	-0.8	0.8	-0.1	-1.8	-1.4	-0.1	0.9	-0.7	-0.3	-1.6	-1.2	-0.7	1.0	0.4	-0.1	-1.2	0.6	1.2	1.1	0.2	-0.5	0.4	0.8	1.4	1.9	0.0	0.9	0.0	0.6	0.3	1.6	1.0	0.8	0.0	0.3	0.2	-0.4	4.9	0.7
Hibernia (HIB)	-0.9	-0.7	1.0	0.0	-2.0	-1.6	-0.4	0.8	0.1	-0.6	-1.5	-1.4	-1.2	0.3	0.6	0.1	-0.9	1.1	1.3	1.3	0.1	-0.5	0.4	0.5	1.0	2.1	0.7	0.6	-0.4	0.4	0.3	2.3	0.9	0.3	0.0	-0.2	-0.7	-0.1	5.7	0.8
Flemish Pass (FP)	-0.6	-0.7	0.4	-0.5	-2.2	-0.8	0.2	1.0	-0.5	-1.4	-1.5	-1.4	-1.5	-0.3	0.3	0.0	-0.3	0.9	1.1	1.0	0.3	-0.2	0.8	1.1	1.8	1.5	0.4	1.0	-0.7	0.7	0.3	1.4	0.4	-0.6	-1.3	-0.7	0.4	-0.7	5.7	0.8
Flemish Cap (FC)	-0.4	-0.7	0.5	-0.6	-2.4	-1.0	0.3	0.6	-0.4	-1.0	-1.4	-1.3	-1.2	-1.0	0.1	0.4	0.0	0.7	1.1	0.7	0.3	-0.3	0.4	1.1	1.9	1.7	0.7	1.0	-0.6	0.8	0.6	1.8	0.7	-0.6	-1.5	-0.9	-0.4	-0.7	7.1	0.9
St.Pierre Bank (SPB)	0.3	-0.5	1.1	0.4	-2.5	-1.4	-0.2	-0.2	-0.5	-0.9	-1.5	-1.3	-0.5	1.1	0.0	-0.1	-1.1	0.7	1.6	1.3	0.1	-0.7	0.1	0.3	1.5	1.4	-0.3	0.8	0.1	0.8	0.2	2.4	1.3	1.2	0.2	1.1	0.4	-0.2	6.1	0.7

Figure 16. Annual normalized anomalies of SST for the NL regions (see boxes Figure 1).

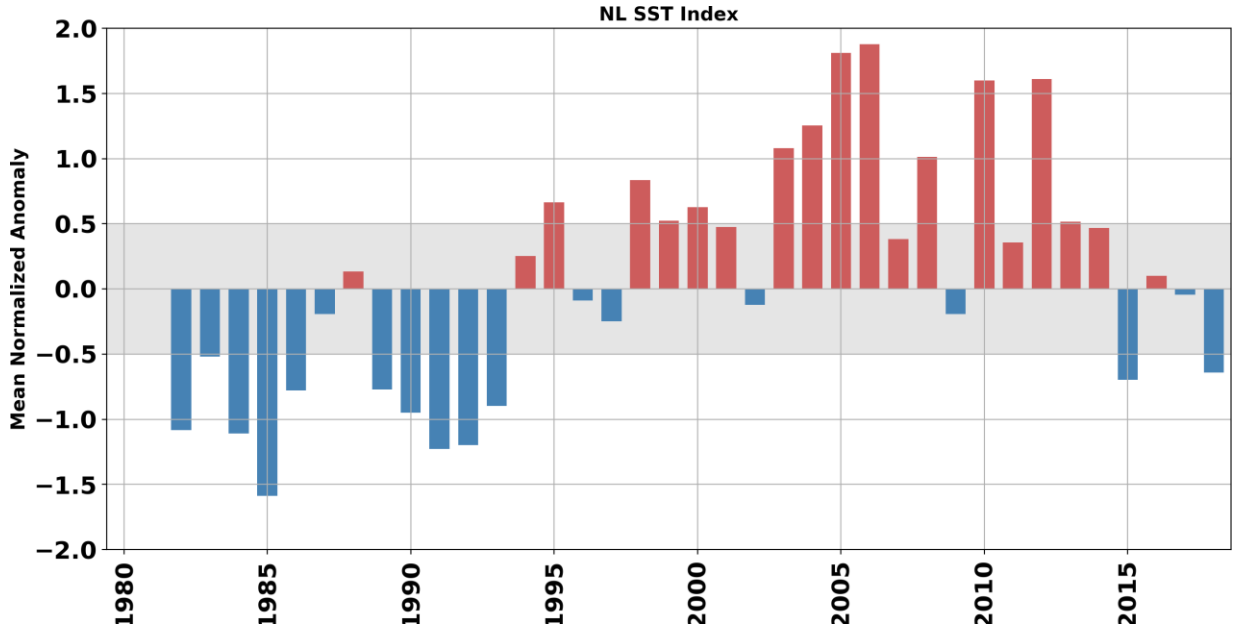

Figure 17. NL SST index (average over all rows of the scorecard of Figure 16). This index contributes to the NL climate index described in the summary (Figure 43).

OCEAN CONDITIONS ON NEWFOUNDLAND AND LABRADOR SHELF

The following section presents results of various ocean parameters (long-term monitoring Station 27, standard hydrographic sections, bottom ocean conditions, etc.).

LONG-TERM OBSERVATIONS AT STATION 27

Station 27 (47°32.8'N, 52°35.2'W), is located in the Avalon Channel off Cape Spear, NL (Figure 1). It is one of longest hydrographic time series in Canada with frequent occupations (near-monthly basis) since 1948. In 2018, the station was occupied 36 times (27 CTD casts, including 16 biogeochemical sampling and 9 XBT). No observations were made in January or February and only one XBT was performed in March. In addition, a total of 202 CTD profiles were collected from an automatic profiling system installed on a surface buoy (type Viking) between July 15th and November 14th 2018 (Figure 18). Station occupation and Viking buoy automatic casts were combined to obtain the annual evolution of temperature and salinity at Station 27, as well as the anomaly compared to the 1981-2010 climatology, shown in Figure 19 and Figure 20. These figures demonstrate the seasonal warming of the top layer (~20m), with temperature peaking in August before being mixed during the fall. The cold intermediate layer (CIL; Petrie et al., 1988), a remnant of the previous winter cold layer and defined as temperature below 0°C (thick black line in Figure 19) is also evident below 100 m throughout the summer. The surface layer is generally freshest between early September and mid-October, with salinities <31 (Figure 20). These low near-surface salinities, generally from early summer to late fall, are a prominent feature of the salinity cycle on the Newfoundland Shelf and is largely due to the melting of coastal sea-ice.

In 2018, the surface layer was colder than normal for most of the spring and early summer, and warmer after mid-August (Figure 19). Except near the surface in the middle of summer, the water column was fresher than normal at all depths and seasons in 2018. Presented in Figure 21 are the annual average temperature (top) and salinity (bottom) over the entire water column (0-176 m). In 2018, the vertically averaged temperature was above normal by about 0.3°C,

coherent with the dominance of warmer than normal temperatures observed since the early 2000s. The vertically averaged salinity was at its freshest state since 1970, a period commonly referred to as the Great Salinity Anomaly in the North Atlantic (Dickson et al., 1988).

The CIL summer (May-July) statistics at Station 27 since 1950 are presented in Figure 22. The striking feature in this figure is the anomalously warm and thin CIL anomaly present from the early 1960s to the mid-1970s. This anomaly is accentuated by the fact that the climatological reference period (1981-2010) encompasses a rather cold period that spanned the mid-1980s to the mid-1990s (see Figure 21). The CIL core depth seems uncorrelated to the temperature difference. After the prevalence of a warm CIL in the early 2010s (with some of the warmest years since the mid-1970s), there has been a cooling trend since about 2014. In 2018, however, the CIL was warmer than normal (mean temperature 1.6 SD above normal).

The monthly mean mixed layer depth (MLD) at Station 27 was also estimated from the density profiles as the depth of maximum buoyancy frequency (*N):*

$$N^2 = -\frac{g}{\rho_0}\frac{\Delta\rho(z)}{\Delta z};$$

with g = 9.8 ms^{-2} as the gravitational acceleration and ρ_0 as a reference density. Values from 2018, relative to the long-term average, are presented in Figure 23. The climatological annual cycle shows a gradual decrease of the MLD between late fall and summer (mixed layer thickest in November-December and shallowest in July-August). In 2018, the MLD was much thicker than normal in April (note that no values are available between January and March) with a mean value of more than 70 m compared to the climatological value of less than 40 m. The MLD was also deeper than normal for May and June but near-normal for the rest of the year, except August where it was shallower. Figure 24 shows a time series of the annual mean values of the MLD (solid gray line) and its 5-year moving average (dashed-black line). In general, there is a strong interannual and decadal oscillation in MLD, although it seems to have a slight increasing trend since the late 1990s. In 2018 however the mean annual MLD was near normal.

Stratification is an important characteristic of the water column since it influences, for example, the transfer of solar heat to lower layers and the vertical exchange of biogeochemical tracers between the deeper layers and the surface. The seasonal development of stratification is also an important process influencing the formation and evolution of the cold intermediate layer on the shelf regions of Atlantic Canada. It essentially insulates the lower water column from the upper layers, thus slowing vertical heat flux from the seasonally heated surface layer.

The stratification index at Station 27 is computed from the density (σ_t) difference between 5 and 50 m for each density profile (i.e., $\Delta\rho/\Delta z$). These values are then averaged by month and the annual anomalies are computed from the available monthly averages (Craig and Colbourne, 2002). The 2018 and climatological evolution of the stratification throughout the year are shown in Figure 25. The stratification is generally weakest between December and April, before rapidly increasing at the onset of spring until it peaks in August. In 2018, the stratification was weaker than normal for most of the year (note that no data are available between January and March), except for September and October where it was normal (see light vs dark blue in Figure 26). The interannual evolution of the stratification anomaly since 1950 is shown in Figure 26. While strong decadal variations are observed, a positive trend is distinguishable since the mid-1970s, with the highest annual anomaly since 1950 observed in 2017 (+0.9 SD). In 2018, the annual stratification was weaker than normal at -0.7 SD. A scorecard of annual standardized anomalies since 1980 of all parameters discussed in this section is presented in Figure 27.

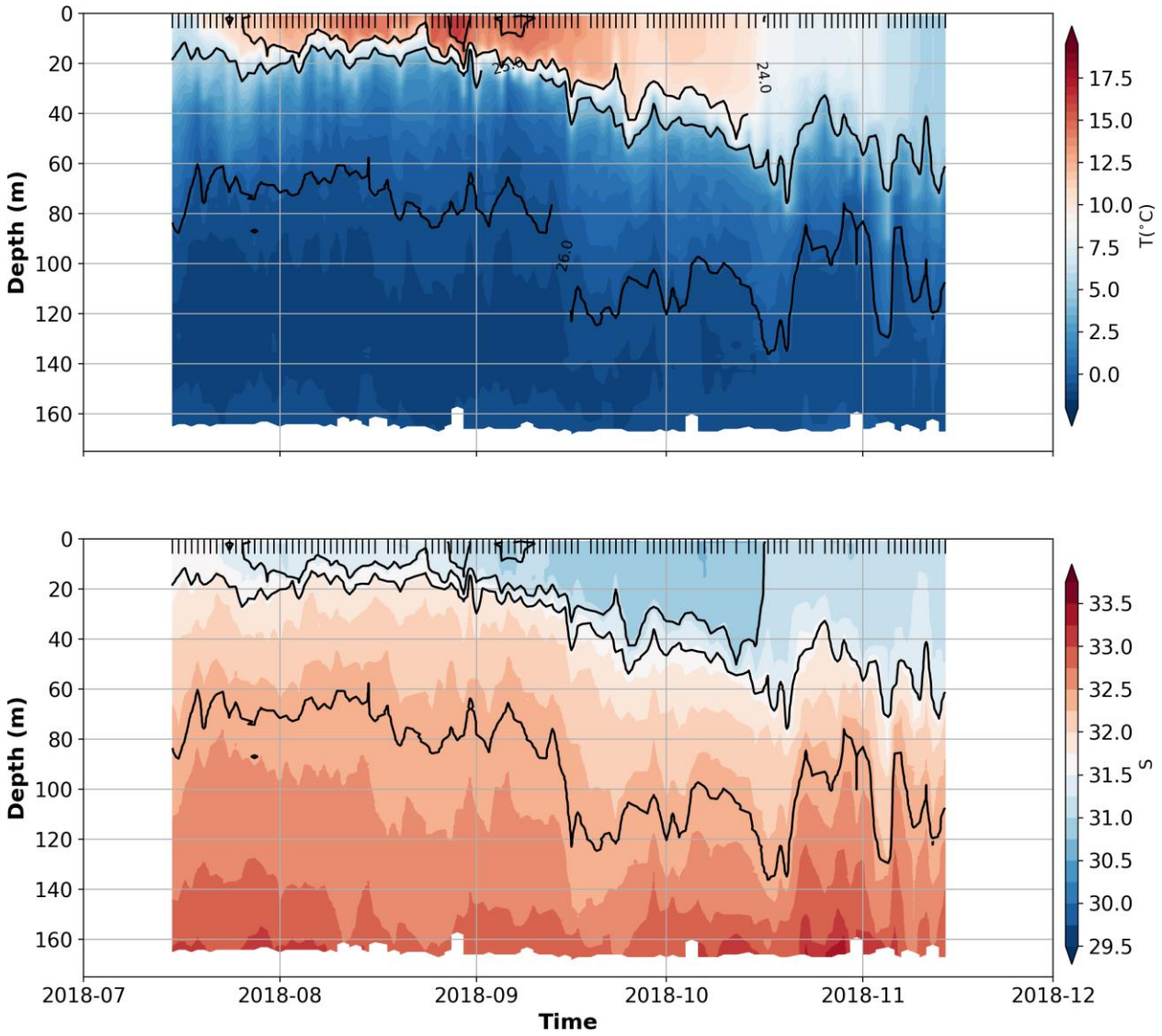

Figure 18. Temperature (top) and salinity (bottom) fields as measured by the Viking buoy automatic profiling system at Station 27. Isopycnals (σ_t, black lines) are identified on top panel. All casts have been averaged as daily mean profiles (marked as black tick marks on the top of the Figure) before being linearly interpolated in time.

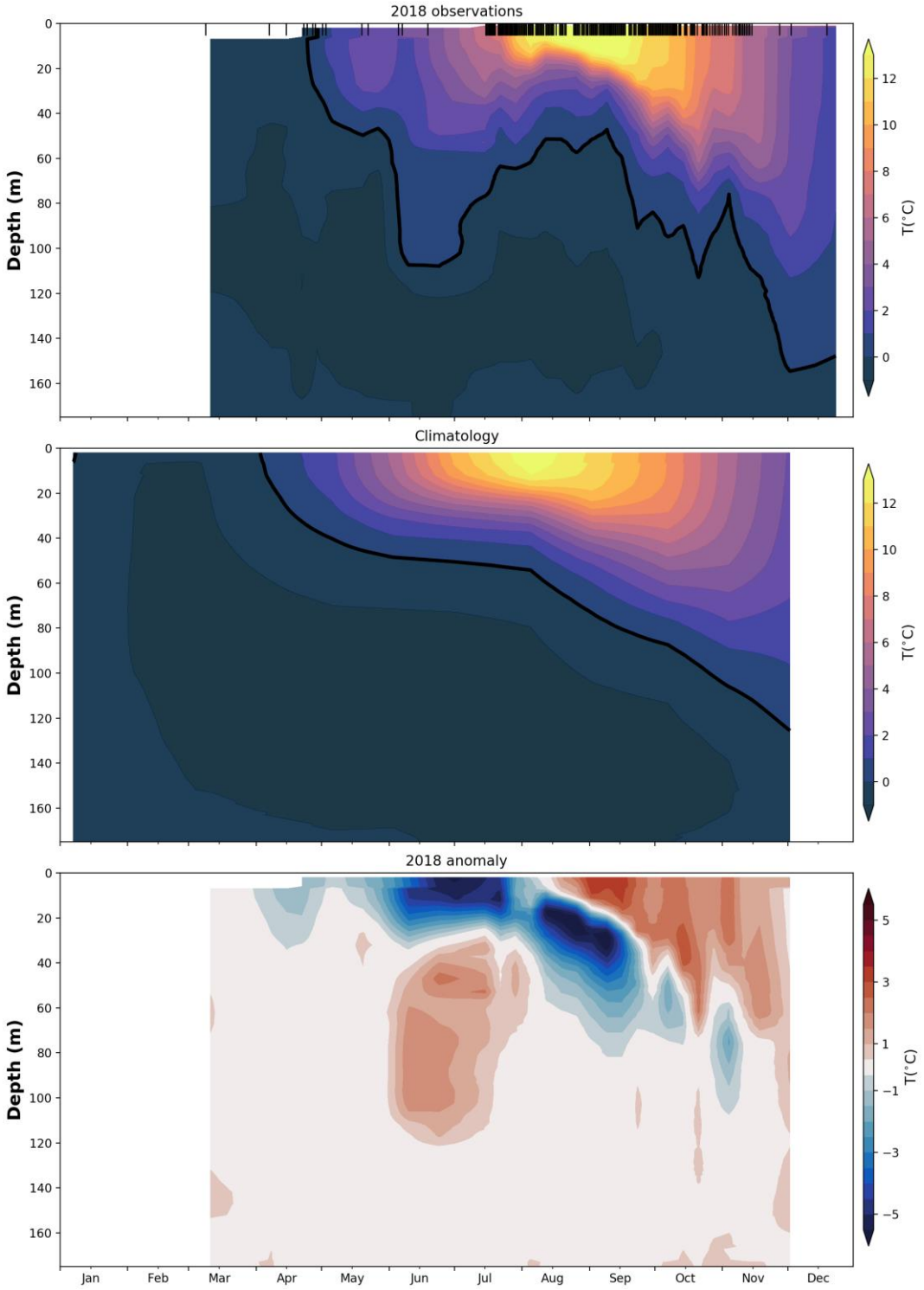

Figure 19. Annual evolution of temperature at Station 27. The 2018 contour plot (top panel) is generated from weekly averaged profiles from all available data, including station occupation and Viking buoy casts (indicated by black tick marks on top of panel). The solid black contour delineates the cold intermediate layer defined as water below 0°C. The 1981-2010 climatology (middle panel) is plotted from monthly-averaged temperature profiles. The anomaly (bottom panel) is the difference between the 2018 field and the climatology.

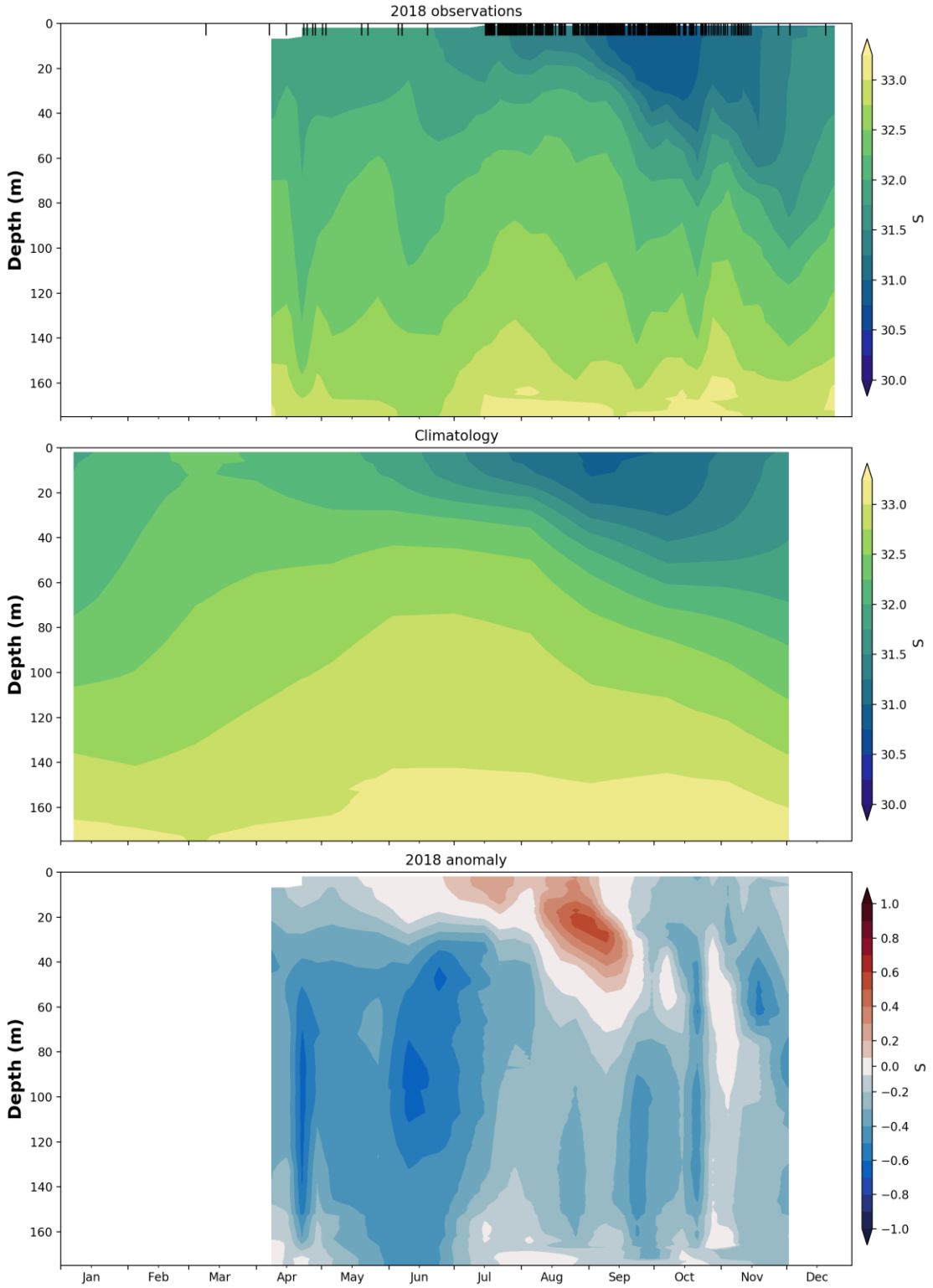

Figure 20. Same as in Figure 19, but for salinity.

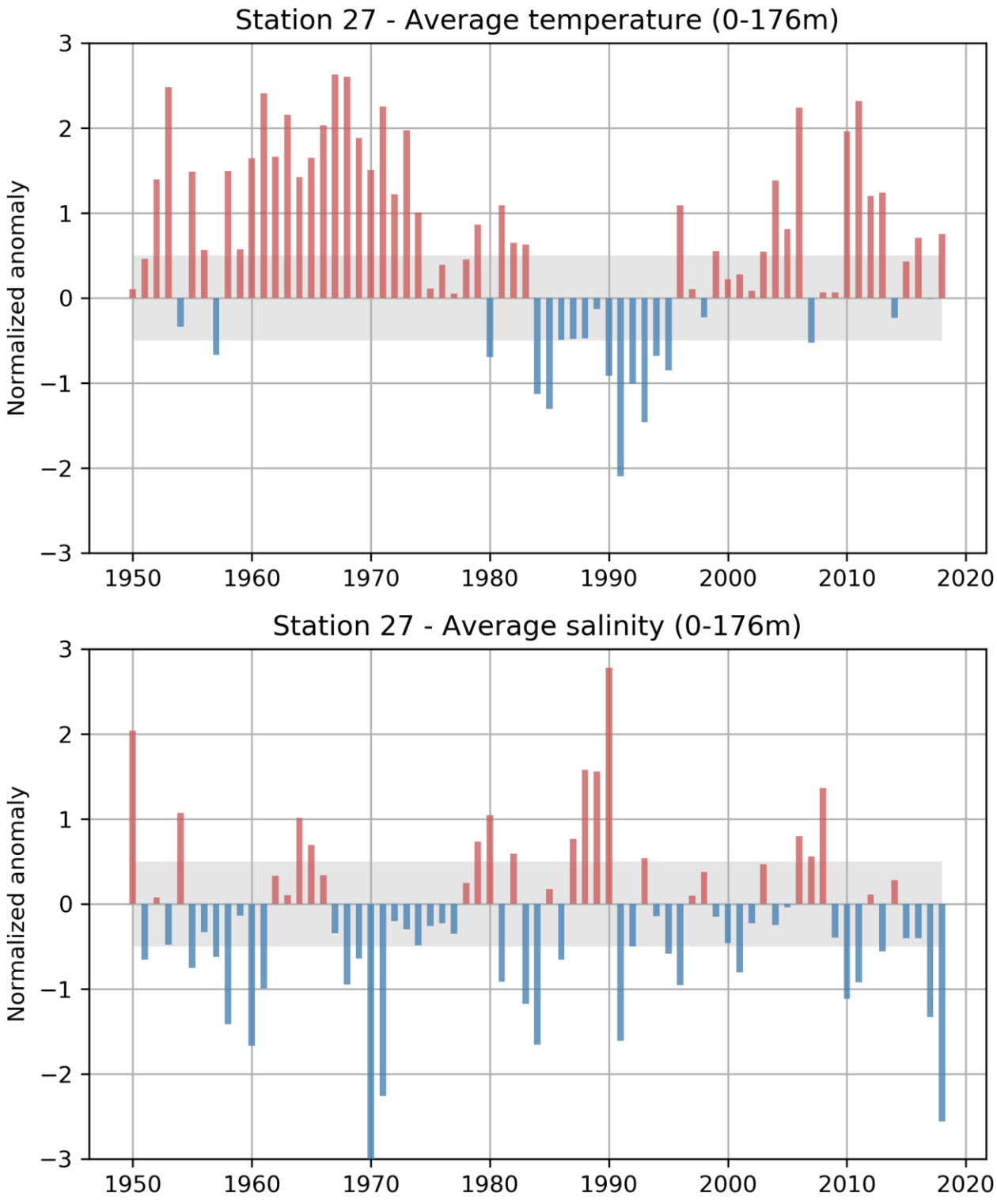

Figure 21. Annual normalized anomaly of vertically averaged (0-176m) temperature (top) and salinity (bottom) at Station 27 calculated from all occupations since 1950. These two time series contribute to the NL climate index described in the summary (Figure 43).

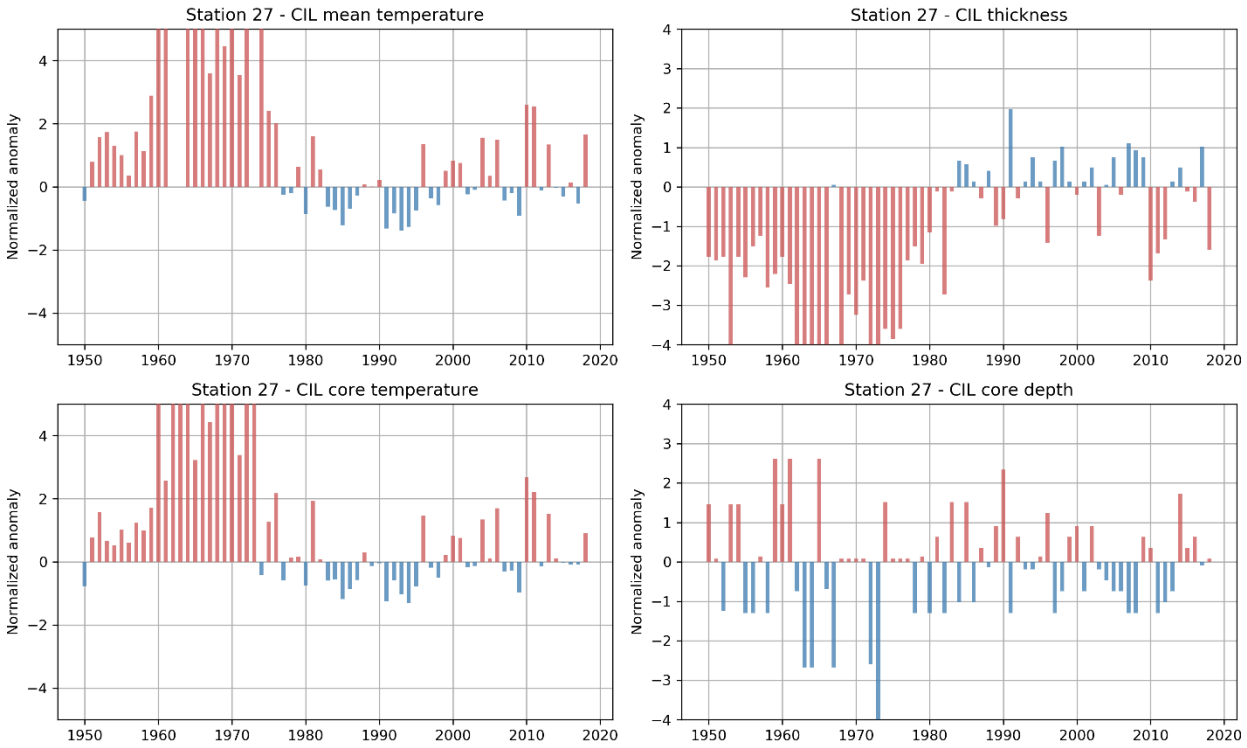

Figure 22. Normalized anomalies of summer (May-July) cold intermediate layer (CIL) statistics at Station 27 since 1950. The top row shows the CIL mean temperature and thickness, while the bottom row shows its core temperature (minimum temperature of the CIL) and its depth. The CIL mean and core temperature anomalies (upper and bottom left) are averaged and contribute to the NL climate index described in the summary (Figure 43).

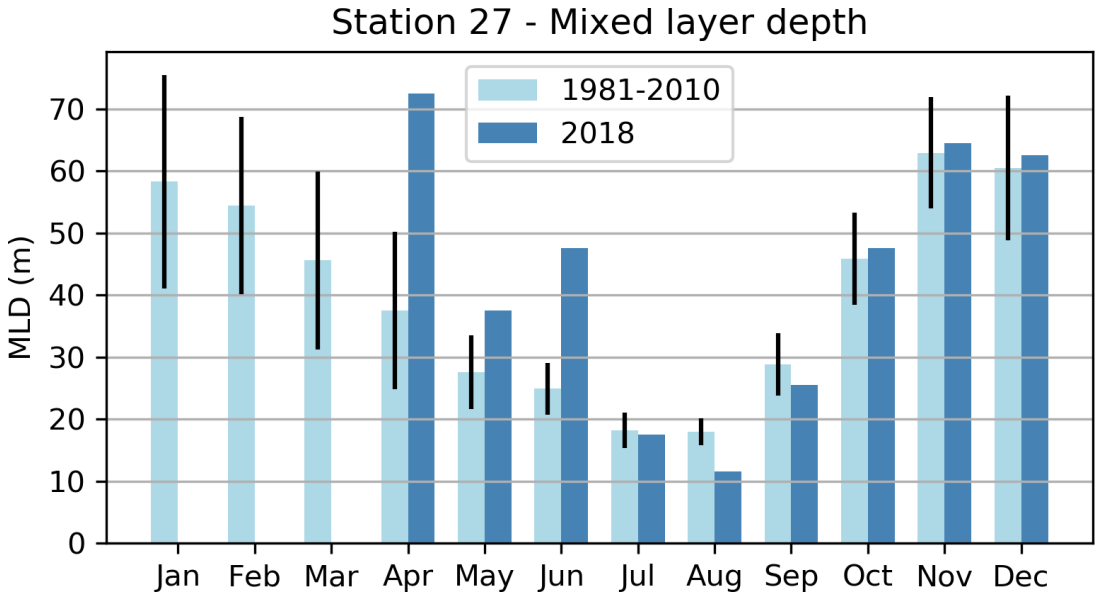

Figure 23. Bar plot of the monthly averaged mixed layer depth (MLD) at Station 27. The 1981-2010 climatology is shown in light blue while the update for 2018 is shown in dark blue. The black lines represent 0.5 SD above and below the climatology.

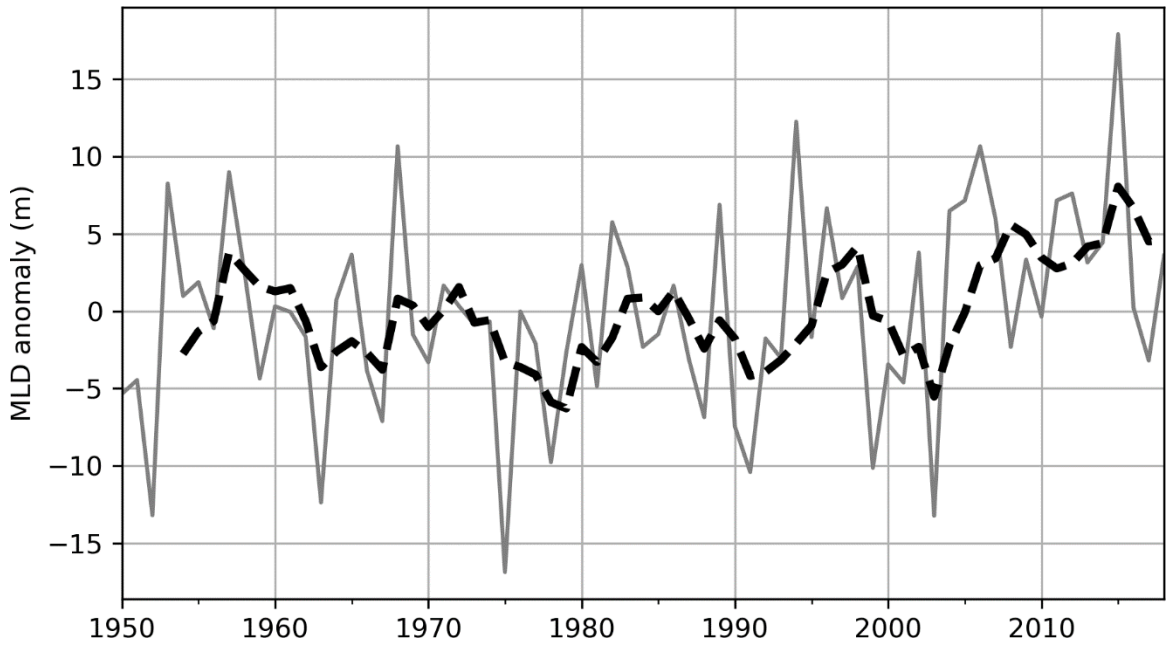

Figure 24. Time series of the annual mixed layer depth (MLD) average at Station 27 since 1950 (gray solid line) and its 5-year running mean (dashed-black line).

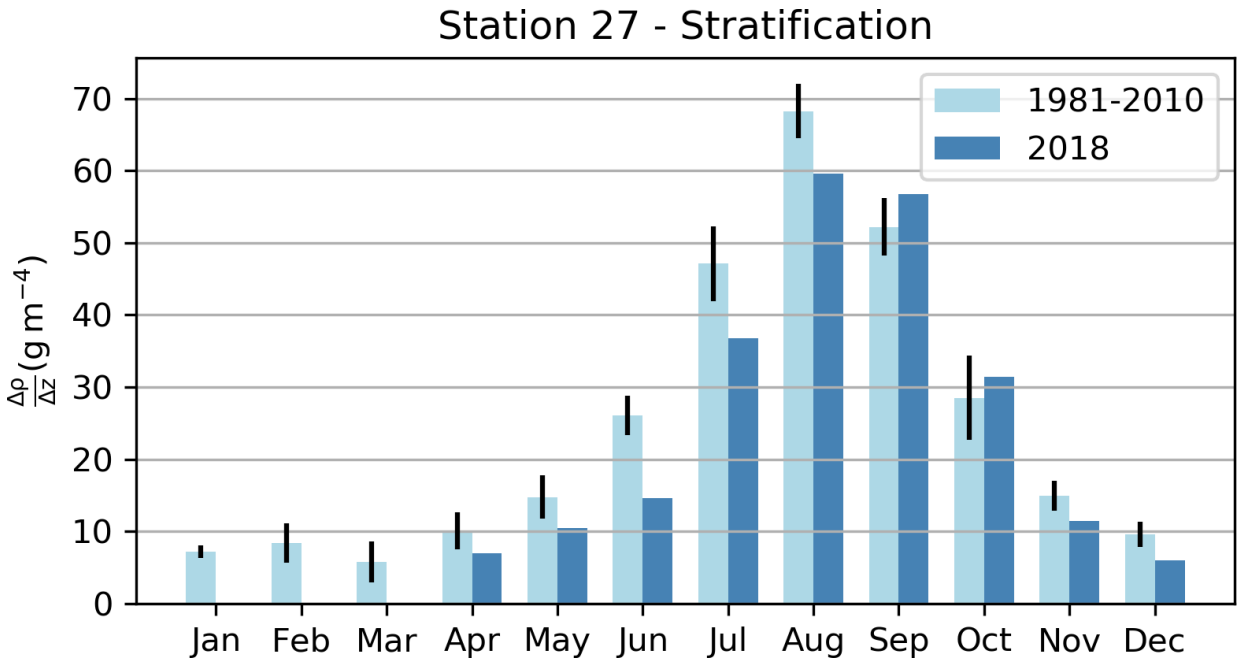

Figure 25. Bar plot of the monthly average stratification (defined as the density difference between 0 and 50 m) at Station 27. The 1981-2010 climatology is shown in light blue while the update for 2018 is shown in dark blue. The black lines represent 0.5 SD above and below the climatology.

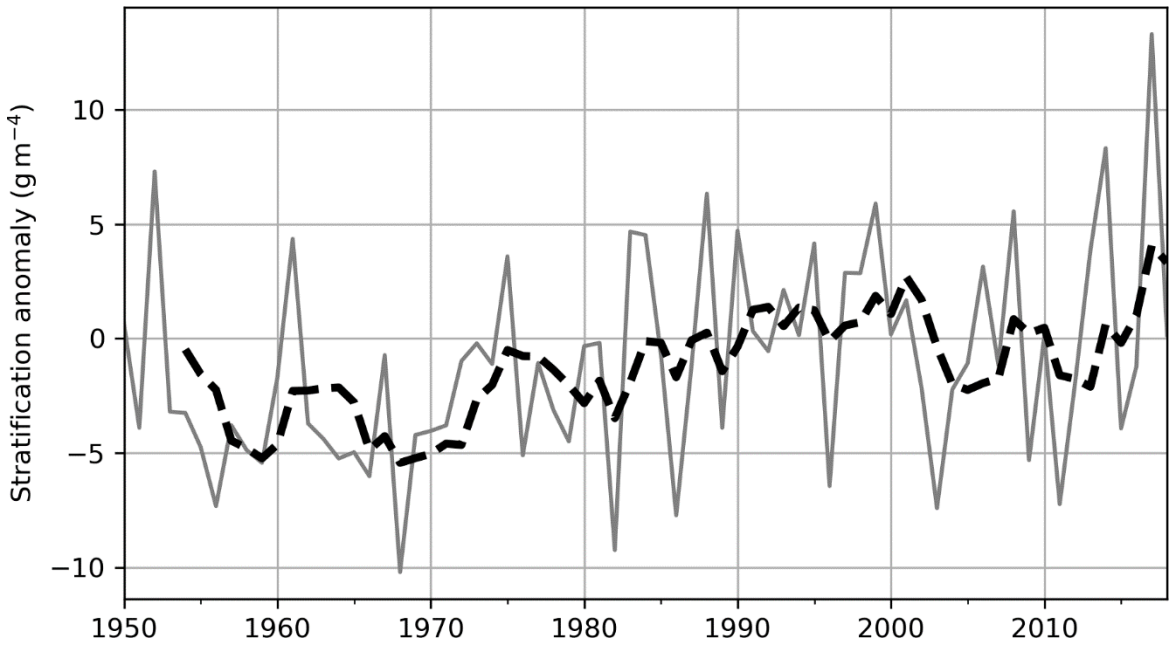

Figure 26. Time series of the annual average stratification at Station 27 since 1950 (gray solid line) and its 5-year running mean (dashed-black line).

	80	81	82	83	84	85	86	87	88	89	90	91	92	93	94	95	96	97	98	99	00	01	02	03	04	05	06	07	08	09	10	11	12	13	14	15	16	17	18	$\bar{x}$	sd
-- Vertically averaged temperature --																																									
Temp 0-176m	-0.7	1.1	0.6	0.6	-1.1	-1.3	-0.5	-0.5	-0.5	-0.1	-0.9	-2.1	-1.0	-1.5	-0.7	-0.8	1.1	0.1	-0.2	0.6	0.2	0.3	0.1	0.5	1.4	0.8	2.2	-0.5	0.1	0.1	2.0	2.3	1.2	1.2	-0.2	0.4	0.7	0.0	0.8	0.4	0.4
Temp 0-50m	-1.6	0.6	-0.6	1.0	-1.2	-1.1	-0.4	-0.4	-0.8	-0.2	-1.0	-2.0	-0.9	-1.2	-0.2	-0.7	0.7	0.3	0.1	0.8	0.1	0.5	0.0	0.8	0.7	0.7	2.6	-1.0	1.0	-0.1	1.9	1.3	1.5	1.7	0.3	0.3	1.4	0.5	0.6	3.2	0.7
Temp 150-176m	-0.1	0.5	-0.1	-0.6	-1.0	-1.6	-0.4	-0.2	-0.3	-0.5	-1.0	-1.6	-1.0	-1.5	-1.3	-0.7	0.7	0.1	0.5	0.7	0.7	0.8	0.2	0.1	2.2	1.6	1.8	0.6	0.1	-0.3	1.5	3.8	1.0	0.9	-0.6	-0.5	-0.4	-0.8	0.7	-1.0	0.3
-- Vertically averaged salinity --																																									
Sal 0-176m	1.0	-0.9	0.6	-1.2	-1.7	0.2	-0.7	0.8	1.6	1.6	2.8	-1.6	-0.5	0.5	-0.1	-0.6	-1.0	0.1	0.4	-0.2	-0.5	-0.8	-0.2	0.5	-0.2	0.0	0.8	0.6	1.4	-0.4	-1.1	-0.9	0.1	-0.6	0.3	-0.4	-0.4	-1.3	-2.6	32.5	0.1
Sal 0-50m	1.0	-0.3	1.4	-1.3	-1.9	0.3	0.6	1.2	1.1	1.6	2.2	-1.9	-0.3	0.1	-0.4	-1.4	-0.4	-0.5	-0.2	-0.4	-0.5	-0.9	0.8	0.9	0.3	0.1	0.1	0.3	0.7	0.0	-1.3	-0.4	0.2	-0.4	-0.4	-0.1	-0.2	-1.9	-1.5	31.9	0.2
Sal 150-176m	1.2	-0.1	0.1	-0.4	-0.2	-0.5	-1.2	0.8	1.9	0.7	3.4	-1.5	-1.5	0.7	-0.3	-0.1	-1.2	0.0	0.6	0.0	-0.1	-0.4	-0.5	-0.8	-0.5	0.0	1.3	0.3	0.8	-0.8	-0.2	-0.4	0.2	-1.0	0.2	-1.0	-1.1	-0.9	-2.3	33.1	0.1
-- Cold intermediate layer (CIL) properties --																																									
CIL temp	-0.4	0.9	0.4	-0.1	-1.0	-0.9	-0.7	-0.6	-0.5	-0.3	0.1	-1.3	-0.7	-1.2	-0.7	-1.2	1.1	-0.3	-0.2	1.0	0.7	1.1	-0.3	-0.2	1.8	0.7	1.2	-0.4	-0.5	-0.9	3.0	3.2	0.3	1.9	0.0	0.0	0.2	-0.4	1.6	-1.0	0.2
CIL core T	-0.3	1.2	0.0	-0.5	-0.8	-1.2	-0.8	-0.6	-0.1	-0.2	-0.3	-1.2	-0.4	-0.8	-1.1	-1.0	1.2	-0.1	-0.2	0.5	1.0	1.0	-0.3	-0.4	1.8	0.2	1.2	-0.1	-0.6	-0.6	3.2	3.1	-0.1	2.3	-0.1	0.4	-0.1	0.0	0.7	-1.4	0.2
CIL core depth	-0.8	-0.8	0.5	-2.1	-1.1	1.9	0.2	0.2	-0.8	-0.8	2.6	-0.8	1.3	0.0	0.5	-0.5	0.5	-0.8	-1.1	0.8	0.2	0.0	0.2	1.0	0.2	-0.3	-0.8	0.8	-1.3	-0.5	0.8	-0.8	-0.5	-1.3	0.8	0.5	0.8	-0.8	0.5	117.4	19.1
CIL thickness	-0.1	-1.2	-1.7	-0.6	1.4	1.3	0.0	0.1	1.0	0.1	-1.1	2.1	-0.5	-0.1	0.4	0.7	-1.1	0.7	0.6	-0.2	-0.2	-0.3	0.5	-1.6	-0.8	0.6	0.3	0.7	0.7	0.7	-2.4	-2.3	-1.3	-0.1	0.1	-0.4	-0.4	0.6	-1.4	127.9	10.9
-- Mixed layer depth (MLD) --																																									
MLD winter	0.6	-0.3	1.0	0.8	0.3	-1.0	-0.6	-0.2		0.3	-0.2	-0.5	0.0	-1.1	0.8	-0.1	0.1	1.2	0.7	-0.2	-0.5	-0.1	0.1	-1.3	0.6	0.8	1.3	0.7	0.3	-1.1	-0.8	0.3	0.6	1.6	1.2	0.8	0.0			54.8	23.4
MLD spring	-0.2	-0.3	-0.3	-0.4	-1.3	0.3	-0.2	0.0	-0.3	0.8	0.4	-0.8	0.3	-0.3	1.1	-0.5	0.0	0.7	-0.8	-0.6	0.6	-0.3	0.4	-0.7	0.5	-0.4	0.2	-0.3	-0.2	0.4	1.9	-0.4	1.5	0.6	0.1	1.3	0.2	0.3	1.7	30.1	10.5
MLD summer	-0.7	-0.5	0.1	0.0	-0.4	0.2	0.6	-0.3	0.0	0.9	0.1	-0.3	0.1	1.0	0.8	1.1	0.3	0.3	-0.8	-0.4	-1.1	0.2	0.0	0.0	-0.8	-0.7	0.2	-0.3	-0.8	0.9	-0.4	1.6	-1.0	-0.1	-1.1	1.4	0.9	-0.6	-0.6	21.7	3.9
MLD fall	0.8	-0.2	-0.8	0.6	0.3	1.1	1.1	-0.2	-0.7	-0.2	-1.5	-0.8	-0.4	0.9	-0.2	0.0	0.9	-0.6	0.4	-0.7	0.0	-0.7	0.1	-0.7	0.3	0.7	-0.4	0.1	0.1	1.3	-0.3	0.8	0.7	-0.6	0.4	0.3	-0.3	0.2	0.1	55.8	13.3
MLD annual	0.1	-0.3	0.1	0.2	-0.3	0.1	0.2	-0.2	-0.3	0.5	-0.2	-0.6	0.0	0.1	0.6	0.1	0.3	0.2	-0.2	-0.5	-0.3	-0.2	0.2	-0.6	0.2	0.0	0.3	0.1	-0.2	0.5	0.3	0.6	0.4	0.2	-0.1	0.9	0.2	0.0	0.4	39.4	6.3
-- Stratification --																																									
strat winter	1.4		0.1		-0.2	0.3	-0.1	-0.6		-0.2	1.5	-0.6	3.9	-1.9	-0.8	-1.5	-0.4	0.4	0.3	0.2	0.6	0.5	0.9	0.0	-0.2	-0.5	-0.3	0.1	0.1	0.2	0.5	0.2	-0.6	-0.2	-0.4	-0.2	-0.8			0.008	0.005
strat spring	-0.7	0.3	-0.5	2.6	1.5	-0.8	-0.3	1.6	0.0	-0.6	-0.3	0.1	-1.1	-0.7	-0.5	1.2	-0.7	0.0	0.6	0.8	-0.4	-0.1	-0.9	-1.0	-0.4	-0.1	0.4	0.2	-0.4	0.1	-0.9	-0.3	-0.6	-0.3	-0.7	-0.2	-0.7	1.4	-1.1	0.017	0.005
strat summer	-0.9	0.3	-0.5	0.8	1.3	0.6	-0.6	-0.7	0.1	-0.6	-0.3	-0.8	-1.4	-0.5	1.2	0.3	-1.3	0.0	0.7	0.9	0.2	0.5	0.1	-0.8	0.2	0.2	0.1	1.0	0.3	-1.2	-0.4	-2.0	0.1	0.9	2.9	-1.1	-0.5	1.8	-0.5	0.055	0.007
strat fall	-1.6	-0.7	-1.6	-0.9	-0.1	-0.5	-1.1	-0.4	0.5	0.3		1.3	0.5	-0.4	0.0	1.7	-0.5	0.3	0.0	0.1	0.5	1.0	-0.9	0.1	-0.3	-0.5	0.5	-0.3	1.2	-0.9	0.2	-0.8	-0.9	-0.1	-0.2	-1.1	1.3	-0.2	-0.5	0.018	0.005
strat annual	-0.5	0.0	-0.5	0.8	0.7	-0.1	-0.5	0.0	0.2	-0.2	-0.1	0.1	-0.2	-0.7	0.0	0.6	-0.7	0.1	0.4	0.6	0.2	0.5	-0.3	-0.4	-0.2	-0.2	0.2	0.2	0.2	-0.4	-0.3	-0.7	-0.5	0.1	0.6	-0.6	-0.1	0.9	-0.7	0.026	0.004

Figure 27. Annual normalized anomalies of hydrographic parameters for Station 27. The different boxes from top to bottom are: vertically averaged temperature and salinity for different depth ranges, cold intermediate layer (CIL) properties, mixed layer depth (MLD), and stratification for the 4 seasons and annual average. The cells are color-coded according to Figure 2. Gray cells indicate absence of data.

STANDARD HYDROGRAPHIC SECTIONS

In the early 1950s, several countries under the auspices of the International Commission for the Northwest Atlantic Fisheries (ICNAF) carried out systematic monitoring along hydrographic sections in Newfoundland and Labrador waters. In 1976, ICNAF normalized a suite of oceanographic monitoring stations along sections in the Northwest Atlantic Ocean from Cape Cod (USA) to Egedesminde (West Greenland) (ICNAF 1978). In 1998 under the AZMP of Fisheries and Oceans Canada, the Seal Island (SI), Bonavista Bay (BB), Flemish Cap (47°N) (FC) and Southeast Grand Bank (SEGB) historical stations were selected as core monitoring sections. The White Bay section (WB) continued to be sampled during the summer as a long time series ICNAF/NAFO section (see Figure 1).

Two ICNAF sections on the mid-Labrador Shelf, the Beachy Island (BI) and the Makkovik Bank (MB) sections, were selected to be sampled during the summer if survey time permitted. Starting in the spring of 2009, a section crossing south-west over St. Pierre Bank (SWSPB) and one crossing south-east over St. Pierre Bank (SESPB) were added to the AZMP surveys.

In 2018, SWSPB and SEGB were sampled during the spring (April) and fall (November / December) surveys, WB, SI, MB and BI during the summer survey (July) and BB and FC during all three surveys (although only the inshore portion of BB was sampled in spring). In this manuscript we present the summer cross sections of temperature and salinity and their anomalies along the SI, BB and FC sections to represent the vertical temperature and salinity structure across the NL Shelf during 2018.

Temperature and Salinity Variability

The water mass characteristics observed along the standard sections crossing the NL Shelf are typical of subpolar waters with a subsurface temperature range of -1.5°C to 2°C and salinities from 31.5 to 33.5. Labrador Slope water flows southward along the shelf edge and into the Flemish Pass and Flemish Cap regions. This water mass is generally warmer and saltier than the subpolar shelf waters with a temperature range of 3°C to 4°C and salinities in the range of 34 to 34.75. Surface temperatures normally warm to between 10°C and 12°C during late summer while bottom temperatures remain <0°C over much of the Grand Banks but increase to between 1° and 3.5°C near the shelf edge below 200 m and in the deep troughs between the banks. In the deeper (>1,000 m) waters of the Flemish Pass and across the Flemish Cap, bottom temperatures generally range from 3°C to 4°C. In general, the near-surface water mass characteristics along the standard sections undergo seasonal modification from annual cycles of air-sea heat flux, wind forced mixing, and the formation and melting of sea ice. These mechanisms cause intense vertical and horizontal temperature and salinity gradients, particularly along the frontal boundaries separating the shelf and slope water masses. The seasonal changes in the temperature and salinity fields along the Bonavista section are presented in Colbourne et al. (2015).

The summer temperature and salinity structures along the Seal Island, Bonavista Bay and Flemish Cap (47°N), hydrographic sections during 2018 are highlighted in Figure 28 to Figure 30. The dominant thermal feature along these sections is the mass of cold and relatively fresh water overlying the shelf. This water mass is separated from the warmer and denser water of the continental slope region by strong temperature and salinity fronts. The cross sectional area (or volume) of the CIL is bounded by the 0°C isotherm and highlighted as a thick black contour in the temperature panels. The CIL parameters are generally regarded as robust indices of ocean climate conditions on the eastern Canadian Continental Shelf.

While the CIL area undergoes significant seasonal variability, the changes are highly coherent from the Labrador Shelf to the Grand Banks. The CIL remains present throughout most of the summer until it gradually decays during the fall as increasing winds deepen the surface mixed layer.

During 2018, temperatures were generally above normal for most of the Seal Island section, except in the offshore waters where they were close to normal (Figure 28, bottom left). Along Bonavista section, temperatures were generally above normal at depth and in coastal surface areas, but colder than normal in subsurface waters on the shelf and offshore at the surface (Figure 29, bottom left). For Flemish Cap section, temperatures were much warmer than normal at depth (more than 2.5°C above normal just above the CIL) and much colder than normal at the surface (by more than 2.5°C below normal in some areas; Figure 30, bottom left). The colder than normal temperature near the surface is in agreement with cold SSTs in most of the NL areas as determined by remote sensing. Warmer than normal temperature at depth also signifies warmer bottom conditions in a large portion of the Grand Banks (see section on bottom observations).

The corresponding salinity cross sections show a relatively fresh upper water layer over the shelf with sources from arctic outflow and the Labrador Shelf with values <33, in contrast to the saltier Labrador Slope water further offshore with values >34 (Figure 28 to Figure 30, right panels). In 2018, subsurface salinities along the Seal Island section were generally lower than normal, except for a localized area above the shelf (50-100km off shore, Figure 28, bottom right). Salinities from Bonavista and Flemish Cap sections show contrasting salinity anomalies between the shelf (fresher than normal) and the offshore (saltier than normal) areas. This is likely due to an unusual extension of the saltier Labrador Current onto the slope in 2018 compared to the climatology (see difference in salinity field between the top two right panels in Figure 29).

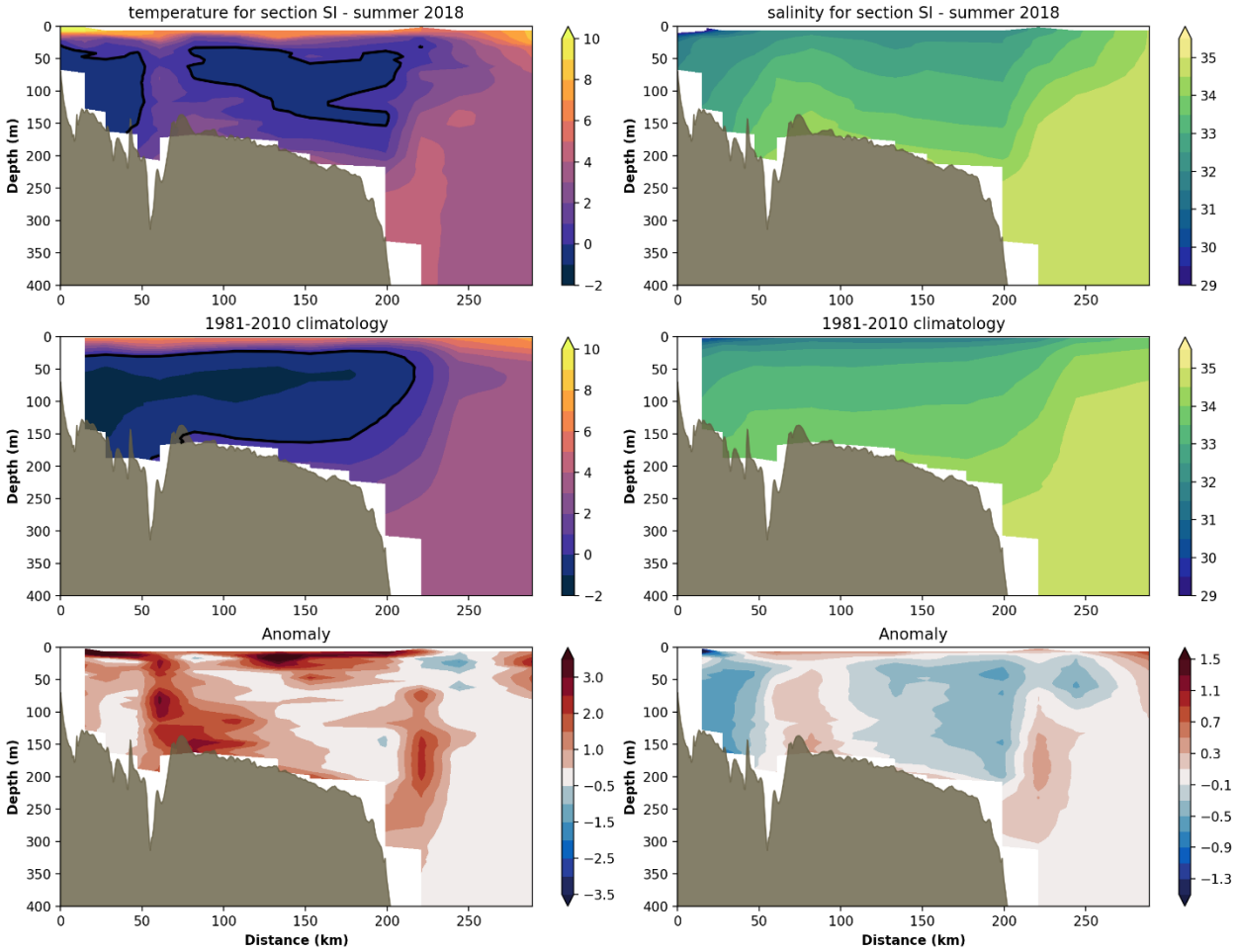

Figure 28. Contours of temperature (°C) and salinity during summer 2018 (top row) and climatological average (middle row) for Seal Island (SI) hydrographic section (see map Figure 1 for location). Their respective anomalies for 2018 are plotted in the bottom panels.

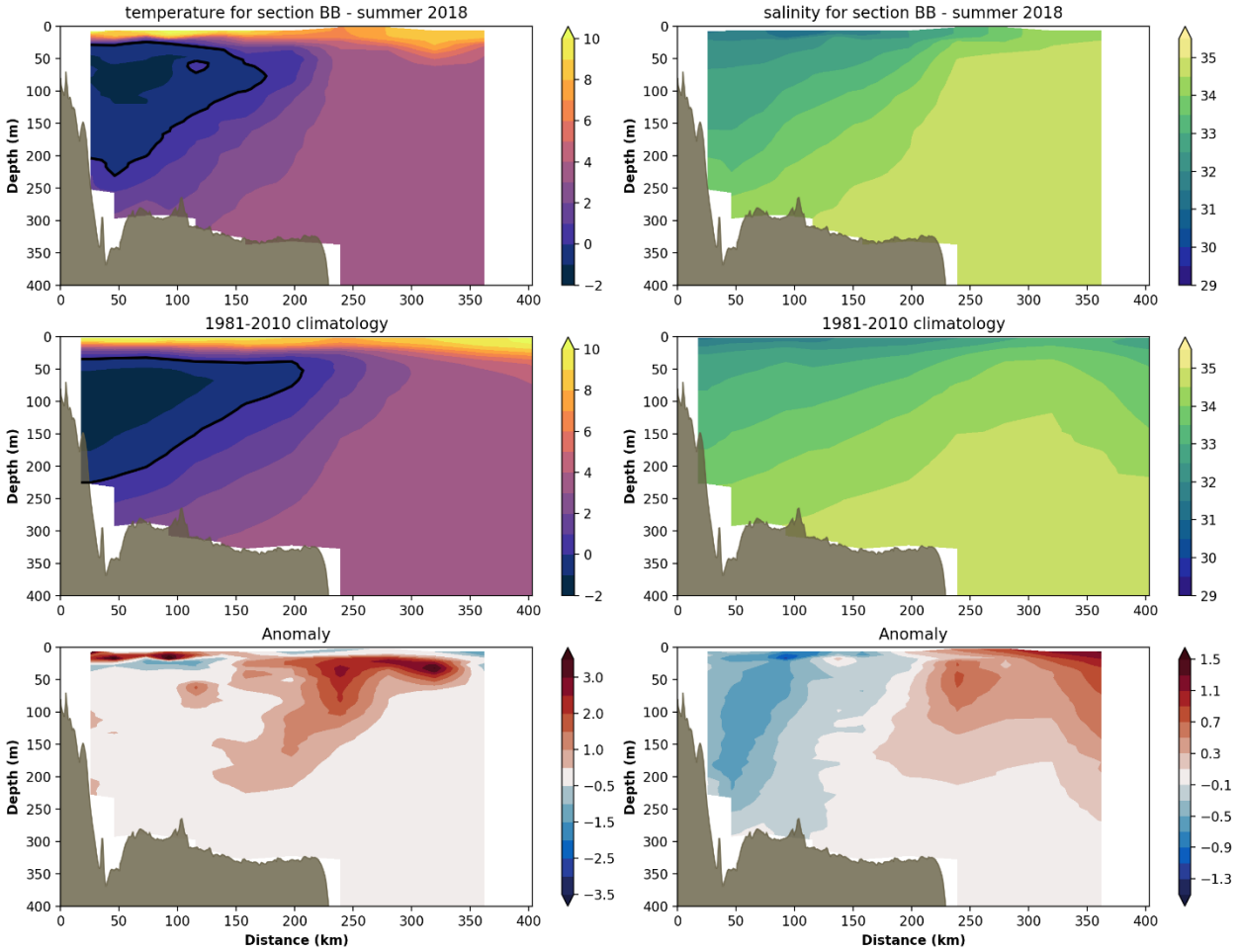

Figure 29. Same as in Figure 28, but for Bonavista (BB) hydrographic section (see map Figure 1 for location).

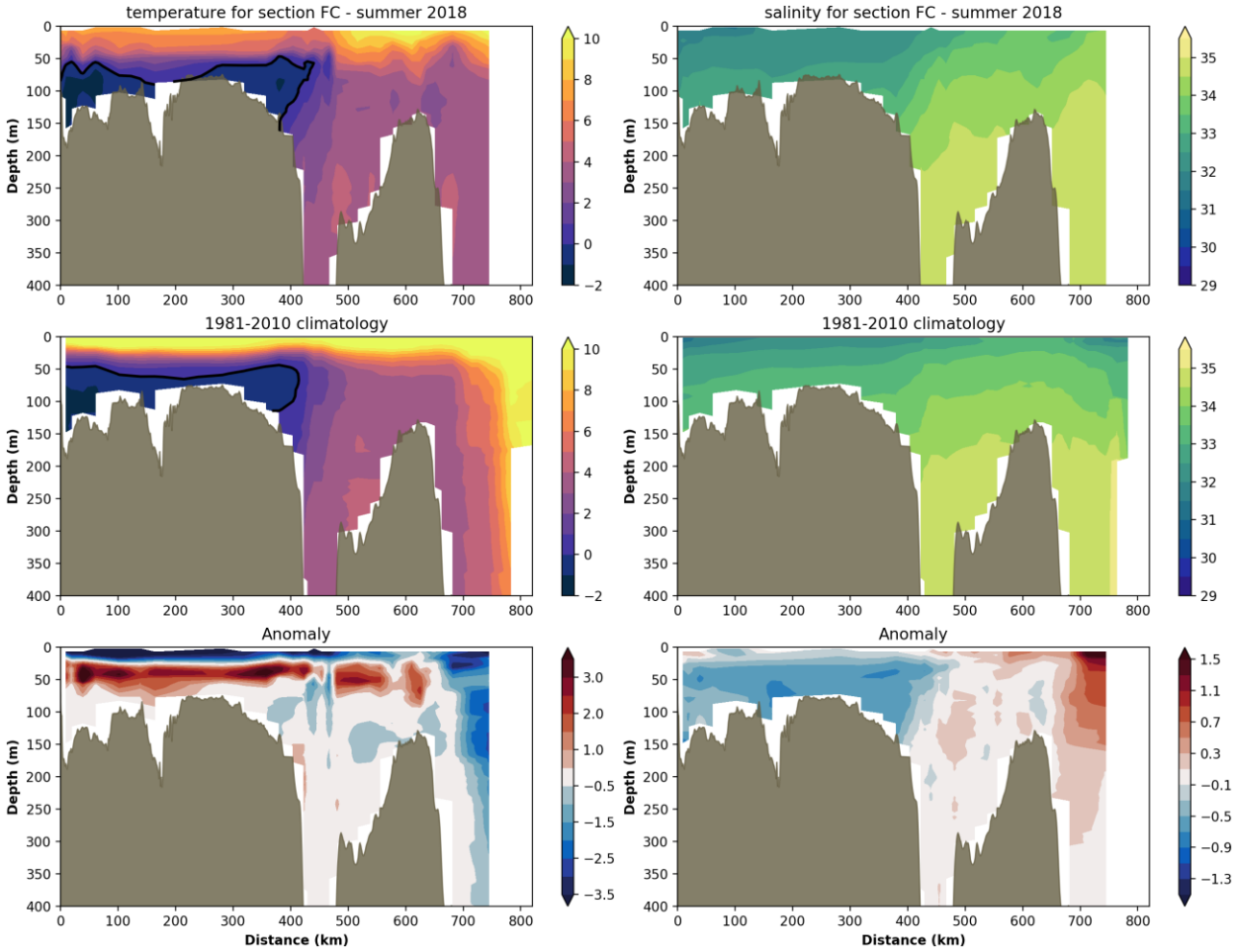

Figure 30. Same as in Figure 28, but for Flemish Cap (FC) hydrographic section (see map Figure 1 for location).

Cold Intermediate Layer Variability

Statistics of summer CIL anomalies for the three sections discussed above (Seal Island, Bonavista and Flemish Cap) are presented as a scorecard in Figure 31. The climatological average cross sectional area of the summer CIL along Seal Island, Bonavista and Flemish Cap sections are 20.3 ± 4.5 km^2, 23.8 ± 8.2 km^2 and 11.7 ± 8.9 km^2, respectively. The averaged anomalies of the CIL core temperature (minimum temperature of this layer) and volume (defined as the cross sectional area) for these three sections are summarized in Figure 32 as a time series going back to 1950. In general, the summer CIL has been predominantly warmer/smaller than average since the mid 1990's, with a cooling trend emerging since about 2012 or 2014. However, the most striking aspect of this long time series is the warm conditions that prevailed in the 1960's (that stands as a unique feature for this nearly 70-year time series, although measurements during this period were largely made from reversing thermometers that might have missed the CIL core), followed by a cold period that lasted from the mid-1980's to the mid-1990's. In 2018, the CIL conditions for two of the three sections studied here have returned to warmer than normal after four years of mostly colder conditions (Figure 31). However, this change seems driven by a shrinking of the CIL (smaller volume) starting from the northern part of the basin with a large negative area anomaly for Seal Island, moderate for Bonavista and

normal for Flemish Cap. Interestingly, while the core temperature along the Seal Island section is 2.5 SD above average, it is normal for Bonavista and Flemish Cap sections.

	-- Seal Island section --																																											
	80	81	82	83	84	85	86	87	88	89	90	91	92	93	94	95	96	97	98	99	00	01	02	03	04	05	06	07	08	09	10	11	12	13	14	15	16	17	18	$\bar{x}$	sd
CIL area (km^2)	-0.1	-1.5	0.3	-0.9	1.6	0.5	-0.3	-0.1	0.1	-3.2	1.5	1.6	1.0	1.3	-0.1	-0.3	0.2	-0.6	0.0	-1.4	-0.2	0.8	-0.1	0.6	-0.9	0.0	-0.2	-0.1	-0.3	0.9	-0.1	-0.9	1.6	-0.7	0.1	1.5	-0.5	1.3	-1.6	20.3	4.5
CIL core (°C)	0.3	0.5	0.0	-1.2	-1.2	-0.9	0.6	0.1	-0.1	3.0	-0.8	-1.1	-0.9	-1.2	-0.7	1.6	-0.4	-0.6	-0.5	0.7	-0.6	0.8	-0.6	0.4	1.8	0.7	0.8	-0.2	-0.7	-0.4	0.9	2.2	-0.5	0.9	-1.2	0.0	-0.4	-0.7	2.5	-1.5	0.2
core depth (m)	0.2	0.6	-0.7	0.6	-0.7	-0.5	1.6	1.7	0.0	1.2	1.6	1.6	-0.3	0.0	1.0	-0.3	-0.9	0.2	0.4	-0.7	-1.5	-1.3	0.0	0.4	-0.2	-1.3	-0.2	0.8	-0.2	-1.3	-1.7	-0.9	0.0	0.0	2.6	-0.2	0.2	-0.9	0.6	70.4	25.4
	-- Bonavista section --																																										
CIL area (km^2)	-0.8	-0.2	-2.8	0.6	2.7	1.2	-0.3	-0.4	0.5	0.2	1.5	2.0	0.1	0.6	0.4	-0.5	-0.1	-0.7	-0.2	-0.3	0.2	-0.4	-0.3	0.2	-1.2	-0.7	-0.9	-0.3	-0.8	0.1	-0.2	-2.0	-0.1	-0.5	1.2	0.7	0.3	0.1	-0.5	23.8	8.2
CIL core (°C)	1.6	0.7	4.1	-1.3	-0.9	-0.7	0.0	0.1	0.6	-0.8	-0.7	-0.9	-0.3	-0.5	-0.8	-0.3	0.4	-0.4	-0.5	-0.2	-0.3	0.1	-0.2	-0.3	1.2	0.4	1.5	0.4	-0.3	-0.6	0.4	1.5	-0.6	0.1	-0.8	-0.7	-0.5	-0.7	0.4	-1.5	0.2
core depth (m)	-0.3	-0.6	0.9	1.3	-1.2	-0.8	0.1	0.5	-0.3	0.3	1.7	0.5	0.7	0.9	0.3	2.7	-0.1	-0.1	-1.0	0.7	0.3	-1.0	1.1	0.3	-0.3	-1.4	-0.6	-1.8	0.1	-1.4	-1.4	0.3	1.1	-0.6	0.7	1.9	-1.0	-0.3	-0.1	90.2	24.8
	-- Flemish Cap section --																																										
CIL area (km^2)	0.2	0.3	-1.3	2.0	1.2	0.9	0.2	-0.4	-0.2	0.8	1.7	1.3	0.3	0.9	-0.4	0.0	-0.3	-0.6	0.9	-0.6	-1.1	-1.3	-0.8	-0.9	-1.0	-0.4	0.0	2.0	-1.0	-1.2	-0.9	-1.1	-1.3	-0.6		0.0	-0.2	-1.3	-0.3	11.7	8.9
CIL core (°C)	-0.4	0.5	2.9	-0.9	-0.3	-0.9	-0.6	-0.7	0.0	-0.8	-0.5	-0.9	-0.7	-0.7	-0.7	-1.4	0.0	-0.3	-0.6	0.4	0.3	3.1	0.2	0.4	0.3	0.1	0.9	0.1	-0.2	0.0	0.9	1.2	0.3	1.1		0.1	0.0	0.0	0.0	-1.3	0.5
core depth (m)	-1.5	-2.1	-0.4	-0.7	-0.1	-0.1	1.6	-0.9	-0.7	-0.9	0.2	-0.9	-0.9	1.3	-0.9	1.0	2.1	0.2	0.7	1.6	-0.1	1.3	-0.1	-0.7	-0.7	-0.9	-0.1	1.1	0.2	-0.9	1.0	-1.2	1.6	1.0		-0.7	-0.1	1.6	1.6	83.4	18.0

Figure 31. Scorecards of the cold intermediate layer (CIL) summer statistics along Seal Island, Bonavista and Flemish Cap hydrographic sections. The CIL area is defined as all water below 0°C (see black contours in Figure 28 to Figure 30), and the CIL core temperature and depth are the minimum temperature of the CIL and the depth at which it is encountered respectively. Color codes for the area and depth have been reversed (positive is blue and negative is red) because they represent cold conditions. Grayed cells indicates absence of data.

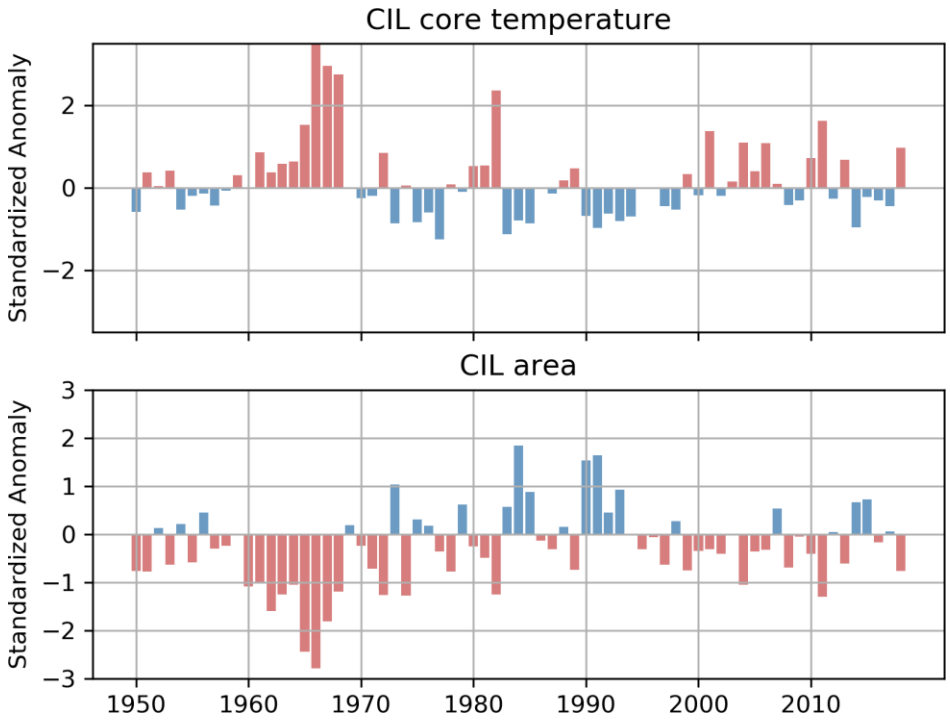

Figure 32. Mean normalized anomalies of the summer CIL core temperature (top) and area (bottom) over Seal Island, Bonavista and Flemish Cap sections since 1950 (values for each separate section since 1980 can be found in Figure 31). The mean summer CIL area for the three sections (bottom) contribute to NL climate index described in the summary (labeled CIL volume in Figure 43).

BOTTOM OBSERVATIONS IN NAFO SUB-AREAS

Canada has been conducting stratified random bottom trawl surveys in NAFO Sub-areas 2 and 3 on the NL Shelf since 1971. Areas within each division, with a selected depth range, were divided into strata, and the number of fishing stations in an individual stratum was based on an area-weighted proportional allocation (Doubleday 1981). Temperature profiles (and salinity profiles since 1990) are available for most fishing sets in each stratum. These surveys provide large spatial-scale oceanographic data sets for the Newfoundland and Labrador Shelf. NAFO Subdivision 3Ps on the Newfoundland south coast and Divisions 3LNO on the Grand Banks are surveyed in the spring, and Divisions 2HJ off Labrador in the north, 3KL off eastern Newfoundland, and 3NO on the southern Grand Bank are surveyed in the fall. The hydrographic data collected on these surveys are routinely used to assess the spatial and temporal variability in the thermal habitat of several fish and invertebrate species. A number of products based on the data are used to characterize the oceanographic bottom habitat. Among these are contour maps of the bottom temperatures and their anomalies, the area of the bottom covered by water in various temperature ranges, etc. In addition, species-specific ‘thermal habitat’ indices are often used in marine resource assessments for snow crab and northern shrimp.

In many previously published CSAS Research Documents (e.g., Colbourne et al. 2017 and before), these data were combined with AZMP hydrographic surveys to derive bottom temperature and salinity. A new method for calculating these parameters was introduced by Cyr et al. (2019). While most of the data presented here were acquired by DFO-NL during multi-species surveys and AZMP hydrographic campaigns, observations are complemented with data from other origins made available by MEDS (surveys from other DFO regions, international oceanographic campaigns, Argo program, etc.).

Moreover, the calculation method of the bottom conditions also differs slightly. While previous calculations consisted of a flat 2D interpolation of the closest observations to the bottom, this new method now considers the bathymetry during the determination of the bottom conditions of the observed fields. For consistency, historical time series presented in this section have been recalculated using the same methodology. Small discrepancies may thus exist between the results presented here and the same quantities reported in previous years.

This new method is similar to the approach presented in reports of the annual physical oceanographic conditions for the Gulf of St. Lawrence (e.g., Galbraith et al. 2019). First, all available annual profiles of temperature and salinity are vertically averaged in 5 m bins and vertically interpolated to fill missing bins. Then, for each season (April-June for spring and October-December for fall), all data are averaged on a regular 0.1° x 0.1° (latitudinal x longitudinal) grid to obtain one seasonal profile per grid cell. Since this grid has missing data in many cells, each depth level is horizontally linearly interpolated. For each grid point, the bottom observation is considered as the data at the closest depth to the GEBCO_2014 Grid bathymetry (version 20141103), to a maximum 50 m difference. Lastly, bottom observations deeper than 1000 m are clipped. This method is applied for all years between 1980 and 2018 from which the 1981-2010 climatology is derived. Anomalies for 2018 are calculated as the difference between annual observations and the climatology.

Spring Conditions

Spring bottom temperature and salinity climatological maps, together with 2018 observations and anomalies for NAFO divisions 3LNOPs, are presented in Figure 33 and Figure 34, respectively (with center panel for station occupation coverage). In 2018, bottom temperatures in 3L were generally below 0°C except in the northern part and near the shelf edge where they ranged from 2°C to 4°C. Over the central and southern areas of the Grand Bank (3NO), bottom temperatures ranged from 0°C on the bank to 6°C on the slopes. Bottom temperature anomalies were slightly warmer than normal over 3LNO where anomalies of 0.5°C to 3.5°C were observed. On St. Pierre Bank (eastern 3Ps), temperatures were generally below 0°C over the shallower shelf and above 5°C in the Laurentian Channel, and bottom temperatures were also warmer than normal by 0.5°C to 2.5°C.

Spring bottom salinities in 3LNO generally range from 32 to 33 over the central Grand Bank, and from 33 to 35 closer to the shelf edge. In 3Ps, salinities were between 32 and 33 over shallower areas and above 34.5 in the Laurentian Channel. In 2018, a widespread fresh water anomaly is observed over the entire 3LNOPs, reaching -0.4 to -0.6 salinity units lower than normal.

Climate indices based on normalized spring temperature anomalies between 1980 and 2018 are shown in a color-coded scorecard in Figure 35. Overall, the colors visually highlight two contrasting periods of this time series: the cold period of the late 80's/early 90's (mostly blue cells) and the warm period of the early 2010's (mostly red cells). This warm period lasted between 2010 and 2013 (2011 being the warmest at 2.4 SD above normal in 3LNO) before returning towards to normal values. Between 2015 and 2017 the bottom area that was covered by <0°C was only -0.1 to 0.1 SD above normal. In 2018, the average bottom temperature for 3LNO was again above normal by 0.5 SD.

Division 3Ps bottom temperatures exhibit some similarities with those from 3LNO, with two periods of warm years, 1999-2000 and 2005-2006, separated by a colder period (2003 is the coldest year on record since 1991 at -1.0 SD). With the exception of 2007 (cold at -0.6 SD) and 2008 (normal), all years between 2005 and 2018 were warmer than normal with the warmest year occurring in 2016 at 1.9 SD above normal. The spring of 2018 was +1.4 SD above normal.

The spring of 2011 had the lowest area of <0°C bottom water of the time series at 1.7 SD below normal. The area of <0°C water on the bottom continued to be below normal in 2018 at (-1.0 SD).

The mean normalized anomaly derived from Figure 35 is presented in Figure 36 as a bar plot integrating all bottom temperature rows of the scorecards (i.e., not considering the thermal habitat areas). An overall increasing trend in bottom temperature is observed from the early 1990s to 2011, although with important interannual variability (e.g., 2003 being the most significant cooling in the last two decades). Bottom temperatures reached record high values in 2011 then experienced a decreasing trend to near-normal values by 2014. On average, 2018 was about 1.0 SD above normal for the entire 3LNOPs.

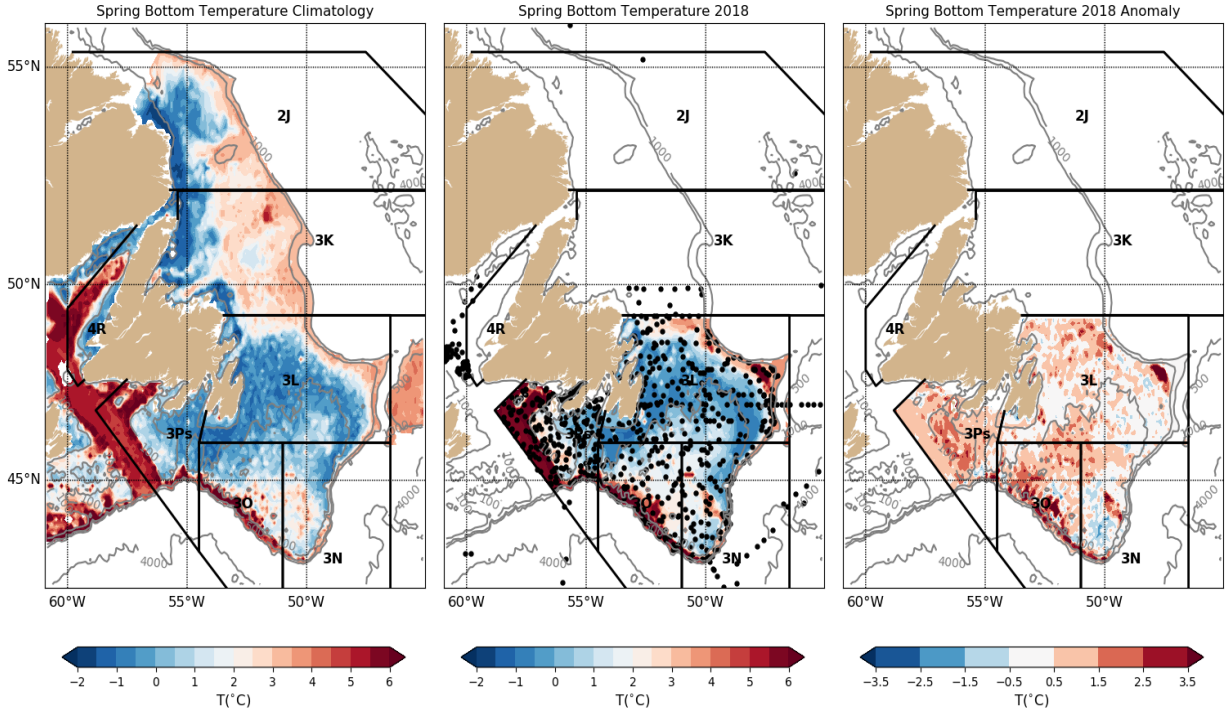

Figure 33. Maps of the mean 1981-2010 spring bottom temperature (left), and spring 2018 bottom temperature (center) and anomalies (right) for NAFO Divisions 3LNOPs only. The location of observations used to derive the temperature field is shown as black dots in the center panel.

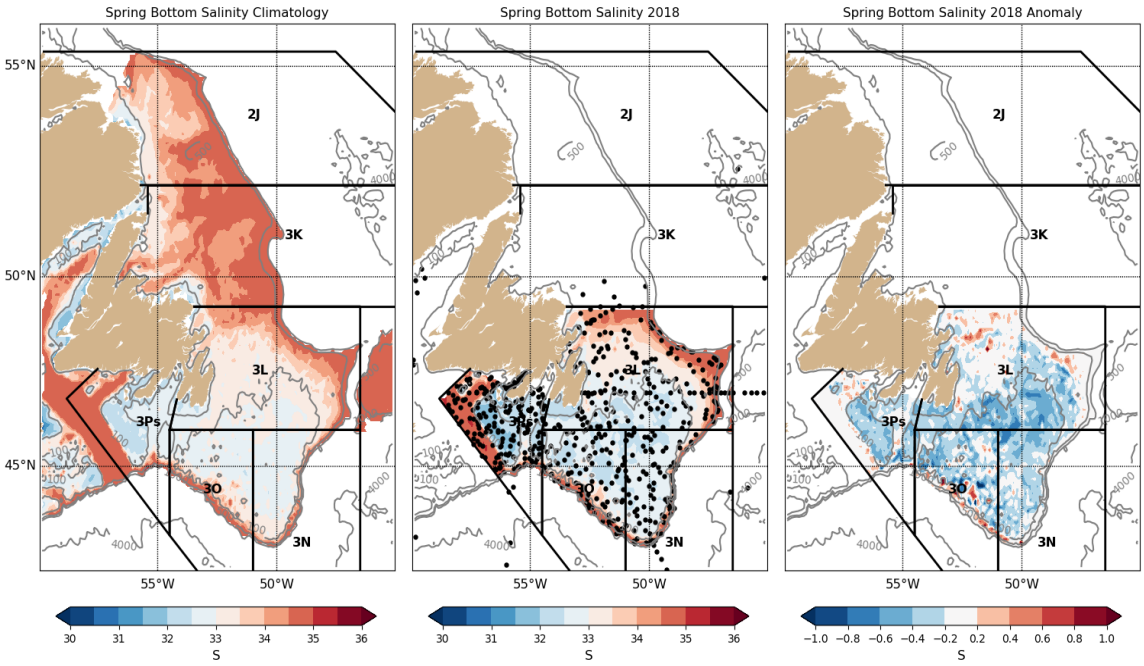

Figure 34. Maps of the mean 1981-2010 spring bottom salinity (left), and spring 2018 bottom salinity (center) and anomalies (right) for NAFO Divisions 2J3KLNO only. The location of observations used to derive the salinity field is shown as black dots in the center panel.

	-- NAFO division 3LNO --																																										
	80	81	82	83	84	85	86	87	88	89	90	91	92	93	94	95	96	97	98	99	00	01	02	03	04	05	06	07	08	09	10	11	12	13	14	15	16	17	18	$\bar{x}$	sd
T_{bot}	0.2	1.7	-0.4	0.7	-0.6	-1.1	-0.9	-0.2	0.3	-1.0	-1.7	-1.7	-1.4	-0.9	-1.2	-0.5	0.3	-0.5	0.8	1.6	0.9	0.4	0.2	-0.7	1.6	0.9	0.9	0.5	0.5	0.5	1.2	2.4	1.7	1.4	-0.2	0.3	0.0	0.2	0.7	0.9	0.6
$T_{bot_{<200m}}$	0.1	1.8	-0.3	1.0	-0.5	-1.1	-1.0	-0.1	0.3	-0.8	-1.7	-1.7	-1.4	-0.9	-1.2	-0.5	0.3	-0.7	0.9	1.7	1.0	0.4	0.1	-0.9	1.5	0.8	0.7	0.4	0.3	0.5	1.1	2.4	1.6	1.4	-0.3	0.2	0.0	0.1	0.5	0.5	0.6
$Area_{>2°C}$	0.1	1.5	-1.1	0.8	-0.4	-1.2	-0.9	-0.1	0.2	-1.1	-1.7	-1.4	-1.5	-0.8	-1.1	-0.2	0.1	-0.5	0.5	1.7	0.7	-0.1	0.1	-0.6	2.0	0.9	0.8	0.7	0.9	0.9	0.6	2.8	1.7	0.8	-0.2	0.8	-0.1	0.3	0.3	64.9	22.7
$Area_{<0°C}$	-0.6	-1.4	-0.1	0.0	0.7	1.0	0.9	0.6	0.2	0.8	1.3	1.5	1.1	1.0	1.0	0.5	-0.4	0.6	-0.9	-1.4	-0.4	-0.4	-0.1	0.7	-2.0	-1.1	-1.8	-0.1	-0.1	0.2	-1.9	-2.2	-1.1	-1.3	0.5	0.1	0.0	-0.1	-0.5	105.9	44.7
	-- NAFO division 3Ps --																																									
T_{bot}	0.7	2.8	0.0	0.5	0.5	-1.3	-0.3	-1.8	0.3	-0.8	-1.8	-1.6	-0.2	-0.5	-0.6	-0.2	0.3	-0.5	0.2	1.0	1.3	-0.4	0.1	-1.0	0.3	1.0	1.0	-0.6	0.3	0.8	0.9	1.5	1.3	1.1	0.9	1.1	1.9	0.7	1.4	2.1	0.6
$T_{bot_{<200m}}$	0.4	3.2	0.2	0.4	0.8	-0.6	-0.2	-1.1	1.1	-0.3	-1.0	-1.0	1.0	-1.4	-1.1	-0.7	0.0	-1.0	0.2	0.9	1.1	-0.7	-0.4	-1.5	0.1	0.9	0.7	-0.7	0.1	0.5	0.4	1.2	0.8	0.7	0.3	0.4	1.0	-0.2	0.8	0.8	0.8
$Area_{>2°C}$	0.4	3.2	0.3	0.8	-0.4	-2.0	-0.4	-1.3	0.3	-0.5	-1.8	-1.7	-0.5	0.0	-0.2	0.3	-0.1	-0.3	0.2	1.3	1.2	-0.4	0.0	-0.4	0.0	0.5	0.7	-0.2	0.5	0.4	0.4	1.1	0.2	0.5	0.4	0.5	0.7	0.1	1.2	26.5	6.3
$Area_{<0°C}$	-0.4	-1.6	-0.4	-0.6	-0.9	0.9	0.1	1.3	-1.2	0.0	0.9	0.6	-0.5	1.6	1.2	1.1	-0.4	1.3	-0.1	-0.7	-1.1	0.6	0.2	2.1	-1.1	-1.4	-1.4	0.6	0.0	-0.3	-0.9	-1.7	-1.4	-1.4	-0.4	-0.8	-1.1	0.2	-1.0	16.3	9.6

Figure 35. Scorecards of normalized spring bottom temperature anomalies for 3LNO (top) and 3Ps (bottom).

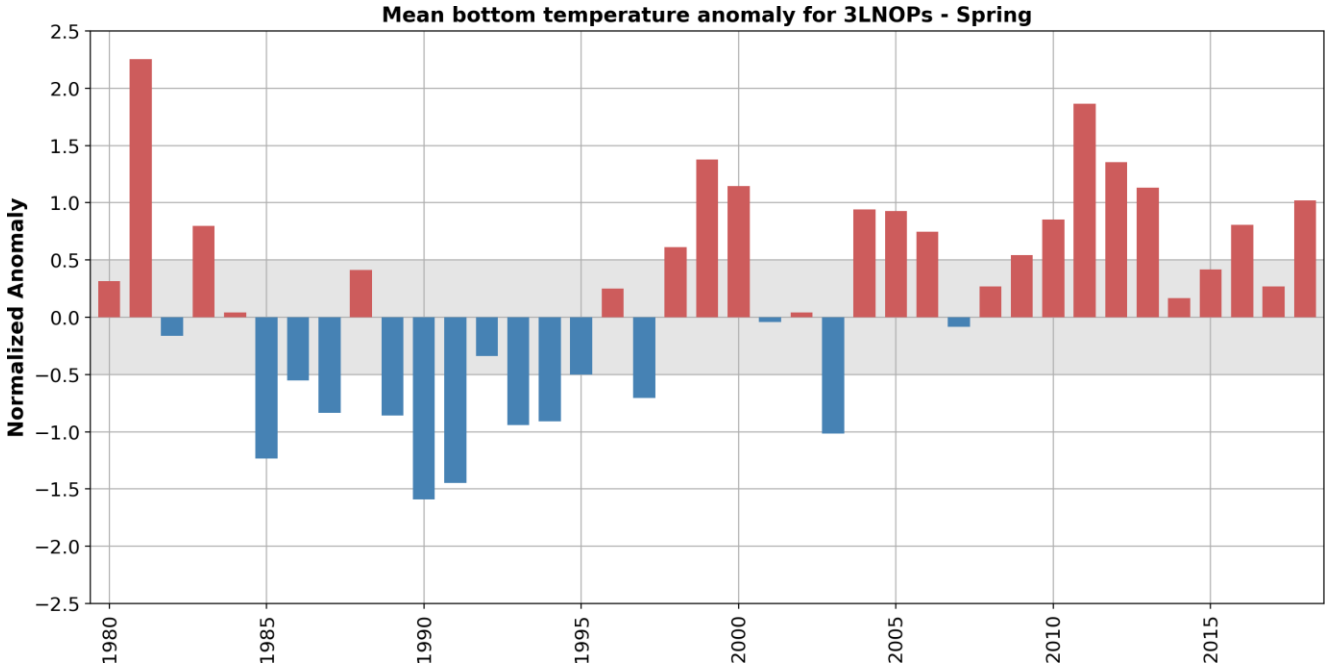

Figure 36. Mean normalized spring bottom temperature anomalies in NAFO Divisions 3LNOPs. The values are the average of the bottom temperature rows in Figure 35 (thermal habitat areas are ignored). This spring bottom temperature time series is further averaged with its fall equivalent (Figure 40) and contributes to the NL climate index described in the summary (Figure 43).

Fall Conditions

Fall bottom temperature and salinity climatological maps, together with 2018 observations and anomalies for NAFO divisions 2J3KLNO, are presented in Figure 37 and Figure 38 respectively (see center panel for station occupation coverage). There is a north-south gradient of bottom temperature anomalies in 2J3KLNO, with warmer than normal conditions in the north: up to +2.5°C in most of 2J; +0.5°C to +2.5°C in 3KL, and a mixture of both colder and warmer than normal in 3NO except for the tail of the Grand Banks which was warmer than normal by 2.5°C.

Bottom salinities in divisions 2J and 3K generally display an inshore-offshore gradient between <33 close to the coast and 34 to 35 at the shelf edge. The Grand Banks bottom salinities range from <33 to 35, with the lowest values on the southeast shoal. In 2018 however, a widespread fresh anomaly decreased the salinity below 33 over most the Grand Banks, with fresh anomalies of more than 0.6 units below normal in most of 3NO (including anomalies close to 1 salinity units in some areas), and fresher by 0.4 units in most of 3L. While 3K was near normal, a fresh anomaly is also observed in the inshore areas of 2J.

Normalized bottom temperature and other derived indices anomalies are presented in the scorecard in Figure 39. While bottom temperature for 2017 was normal in 2J3K and below normal in 3LNO (first negative occurrence in a decade), they are above normal and normal in 2018, respectively.

The mean normalized anomaly derived from Figure 39 is summarized in Figure 40 as a bar plot integrating all rows of the scorecard, except the thermal habitat >2°C. Presented this way, the figure shows the low frequency patterns (~15 year half-cycle) of colder temperatures between the early 80's to the mid-90's, followed by a warmer period until the late 2010's. Since the record high in 2011 and warm conditions in 2016, temperatures have decreased significantly to near-normal values in both 2014 and 2015, and to normal in the spring and below normal during the fall of 2017 (coldest since 1994, as mentioned above). In 2018 however, bottom temperatures returned to above normal conditions at 0.8 SD for 2J3KLNO, the warmest year since the record high temperature in 2011.

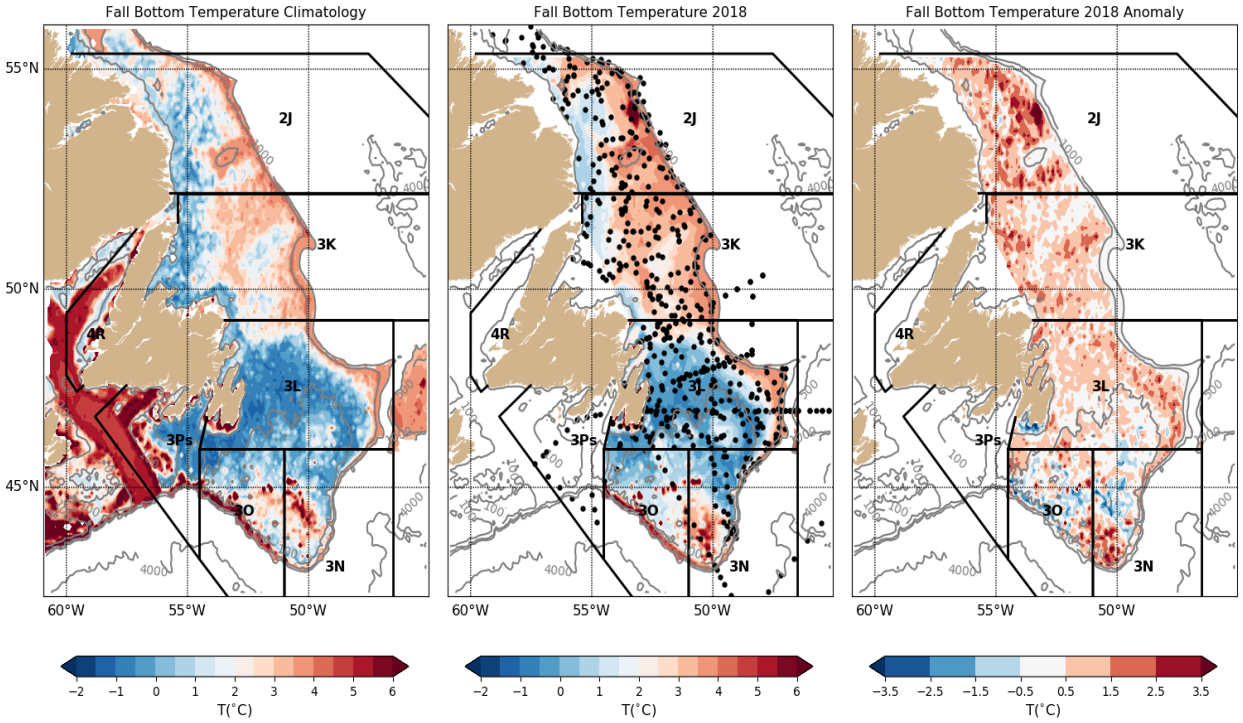

Figure 37. Maps of the mean 1981-2010 fall bottom temperature (left), and fall 2018 bottom temperature (center) and anomalies (right) for NAFO Divisions 2J3KLNO only. The location of observations used to derive the temperature field is shown as black dots in the center panel.

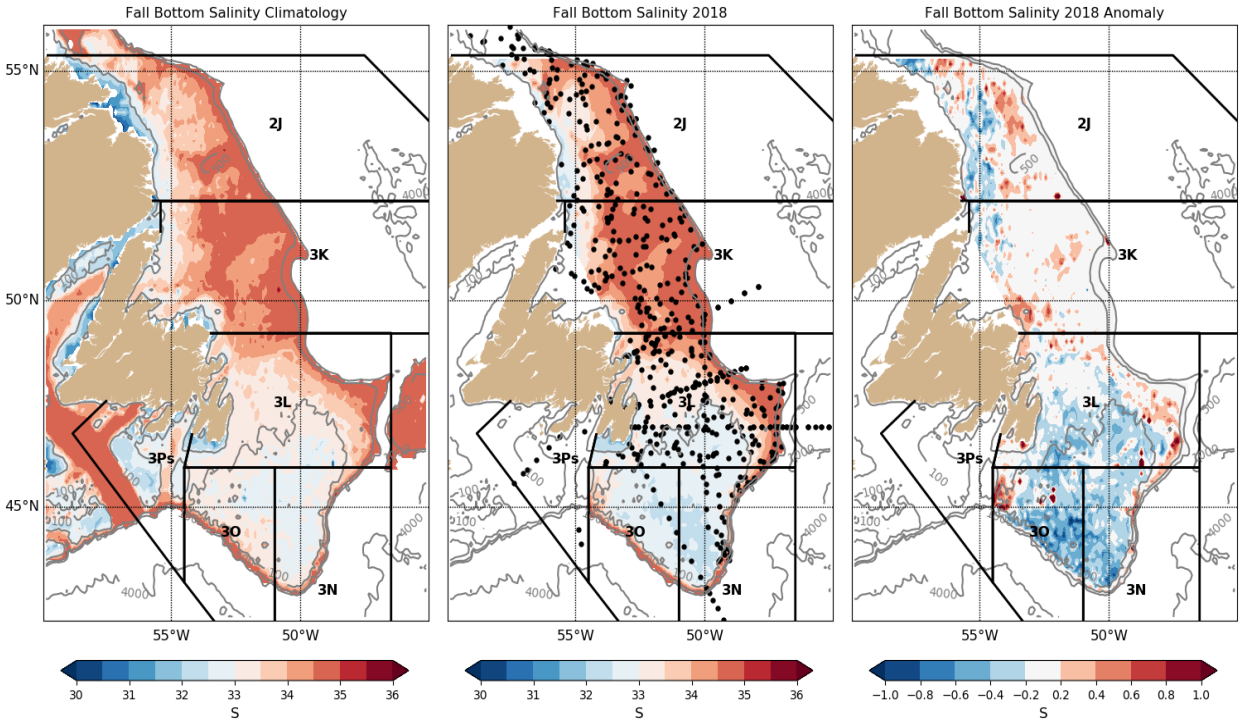

Figure 38. Maps of the mean 1981-2010 fall bottom salinity (left), and fall 2018 bottom salinity (center) and anomalies (right) for NAFO Divisions 2J3KLNO only. The location of observations used to derive the salinity field is shown as black dots in the center panel.

	80	81	82	83	84	85	86	87	88	89	90	91	92	93	94	95	96	97	98	99	00	01	02	03	04	05	06	07	08	09	10	11	12	13	14	15	16	17	18	x̄	sd
	-- NAFO division 2J --																																								
T_{bot}	-0.2	0.3	-1.1	-0.9	-1.9	-1.5	0.3	-1.2	0.1	-0.4	-1.1	-0.7	-1.4	-1.4	-0.8	0.0	0.7	0.4	0.4	0.7	0.1	0.9	0.6	1.0	1.3	1.4	0.1	1.5	0.4	0.5	1.8	1.8	0.4	0.4	-0.1	-0.1	0.6	0.2	1.1	2.0	0.6
$T_{bot_{<200m}}$	0.1	0.4	-0.8	-1.2	-1.8	-1.2	0.4	-1.2	0.1	-0.4	-0.9	-0.9	-1.5	-1.4	-0.8	0.0	0.8	0.3	0.2	0.8	0.0	1.0	0.7	1.0	1.1	1.5	-0.3	1.5	0.2	0.5	1.8	2.0	0.2	0.1	-0.5	-0.3	1.1	0.1	1.0	0.7	0.8
$Area_{>2°C}$	0.0	0.2	-1.4	-0.5	-1.4	-1.3	0.3	-0.9	0.0	-0.7	-1.0	-0.6	-1.0	-1.1	-0.7	-1.6	1.0	0.6	0.3	0.2	0.2	0.9	0.7	1.0	1.2	1.6	0.2	1.8	-0.1	0.1	2.0	2.2	0.0	0.2	-0.1	0.0	0.6	0.1	0.9	46.4	16.3
$Area_{<1°C}$	0.1	-0.4	1.2	1.1	1.5	1.3	-0.5	1.4	-0.5	0.5	1.2	1.0	1.2	1.4	0.9	-1.0	-0.7	-0.4	-0.2	-1.1	0.1	-1.0	-0.7	-1.1	-0.9	-1.5	0.3	-1.4	0.1	-0.4	-1.5	-1.5	0.1	0.0	0.4	0.3	-1.4	0.0	-0.9	26.1	17.0
	-- NAFO division 3K --																																								
T_{bot}	0.1	0.1	-0.2	-0.5	-1.1	-2.0	-0.1	-0.9	-0.3	-0.2	-1.6	-0.7	-1.6	-1.6	-1.1	-0.6	0.1	0.7	0.6	1.0	0.6	0.3	0.8	1.0	1.6	1.1	0.4	1.2	0.9	0.5	1.7	2.3	0.6	0.7	0.0	0.3	0.0	-0.3	0.9	2.4	0.5
$T_{bot_{<200m}}$	0.3	0.1	-1.4	-1.2	-1.4	-1.3	0.4	-1.1	-0.5	-0.3	-1.1	-1.0	-1.1	-1.3	-0.9	0.5	0.9	0.2	0.0	0.8	0.0	0.7	0.9	1.1	1.5	1.2	0.2	1.4	0.2	0.3	2.2	2.0	0.5	0.1	-0.3	0.3	1.3	0.1	1.2	0.2	0.8
$Area_{>2°C}$	0.1	0.4	-0.1	-0.7	-0.9	-2.1	0.2	-0.9	-0.3	-0.4	-1.5	-0.5	-1.4	-1.5	-1.2	-0.9	0.0	0.9	0.8	0.9	0.7	0.2	1.1	0.8	1.3	1.2	0.4	1.1	0.9	-0.2	1.8	1.6	0.4	0.8	-0.2	0.3	-0.3	-0.4	1.1	73.4	14.9
$Area_{<1°C}$	-0.1	-0.2	0.1	0.7	0.9	2.0	-0.8	0.3	-0.2	-0.1	2.1	0.9	1.4	1.9	1.3	-0.2	-0.8	-0.3	-0.2	-0.6	0.0	-0.4	-0.9	-1.0	-1.4	-1.2	0.0	-1.2	-0.2	-0.1	-1.6	-1.6	-0.2	-0.5	0.1	-0.3	-1.0	0.3	-1.2	17.5	10.3
	-- NAFO division 3LNO --																																								
T_{bot}	0.5	0.0	1.3	0.3	-0.4	-1.1	0.2	-0.7	-1.1	0.4	-1.0	-1.5	-1.4	-2.2	-1.4	-0.2	0.2	0.1	1.0	2.2	-0.2	0.3	0.2	-0.1	1.2	0.5	0.8	0.1	-0.4	0.8	1.8	3.1	0.7	0.9	0.5	0.1	0.7	-1.0	0.4	1.1	0.4
$T_{bot_{<200m}}$	0.8	0.1	1.6	0.4	-0.3	-0.9	0.4	-0.7	-1.0	0.4	-0.7	-1.4	-1.1	-2.2	-1.4	0.0	0.4	-0.1	0.9	2.3	-0.5	0.2	0.0	-0.3	1.0	0.4	0.8	-0.1	-0.8	0.8	1.8	3.1	0.6	0.9	0.6	-0.2	0.7	-1.1	0.3	0.7	0.5
$Area_{>2°C}$	0.2	-0.1	0.6	0.7	0.3	-1.4	0.3	-0.6	-1.6	0.9	-1.0	-1.0	-1.4	-1.9	-1.3	-0.4	0.0	0.0	1.3	2.6	0.1	0.2	-0.1	-0.2	1.0	0.4	0.4	0.1	-0.5	0.8	1.5	2.9	1.0	1.1	0.9	0.3	0.8	-0.7	0.0	71.2	20.0
$Area_{<0°C}$	-1.0	0.7	-0.1	0.8	1.1	0.2	-0.3	0.3	0.2	-0.1	0.5	1.5	1.2	2.2	1.5	-0.5	-0.2	0.1	-0.6	-1.7	0.7	-0.2	-0.7	-0.2	-2.3	-0.8	-1.4	-0.1	0.3	-0.3	-1.7	-3.4	0.0	-0.3	-0.2	-0.1	0.1	1.3	-0.8	100.9	27.2

Figure 39. Scorecards of normalized fall bottom temperature anomalies for 2J (top), 3K (middle) and 3LNO (bottom).

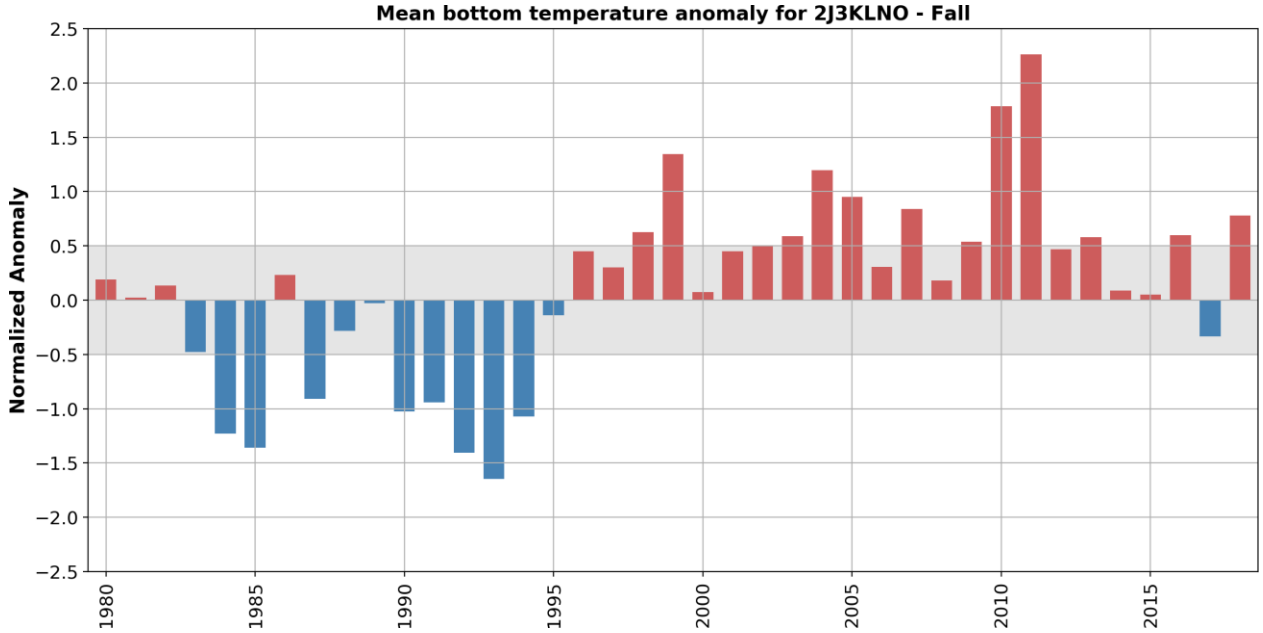

Figure 40. Mean normalized fall bottom temperature anomalies in NAFO Divisions 3LNOPs.The values are the average of all rows in Figure 39, except for the thermal habitat >2°C. This fall bottom temperature time series is further averaged with its spring equivalent (Figure 36) and contributes to the NL climate index described in the summary (Figure 43).

LABRADOR CURRENT TRANSPORT INDEX

The circulation in NL region is dominated by the south-eastward flowing Labrador Current, which floods the eastern shelf areas with cold and relatively fresh subpolar waters (Figure 41). This flow can significantly affect physical and biological environments off Atlantic Canada on seasonal and interannual time scales. The shelf current originates near the northern tip of Labrador where outflow through Hudson Strait combines with the eastern Baffin Island Current and flows southeastward along the Labrador coast where it is strongly influenced by the seabed topography, following the various cross shelf saddles and inshore troughs. A separate offshore branch flows southeastward along the western boundary of the Labrador Sea. This current is part of the large-scale Northwest Atlantic circulation consisting of the West Greenland Current that flows northward along the West Coast of Greenland, a branch of which turns westward and crosses the northern Labrador Sea forming the northern section of the Northwest Atlantic subpolar gyre.

Further south, near the northern Grand Bank, the inshore branch becomes broader and less defined. In this region, most of the inshore flow combines with the offshore branch and flows eastward, with a portion of the combined flow following the bathymetry southward around the southeast Grand Bank, and the remainder continuing east and southward around the Flemish Cap. A smaller inshore component flows through the Avalon Channel and around the Avalon Peninsula, and then westward along the Newfoundland south coast. Off the southern Grand Bank the offshore branch flows westward along the continental slope, some of which flows into the Laurentian Channel and eventually onto the Scotian Shelf. Additionally, there are strong interactions between the offshore branch of the Labrador Current and large-scale circulation. A significant portion of the offshore branch combines with the North Atlantic Current and forms the southern section of the subpolar gyre. Further east, the Flemish Cap is located in the confluence zone of subpolar and subtropical western boundary currents of the North Atlantic. Labrador Current water flows to the east along the northern slopes of the Cap and south around the eastern slopes of the Cap. In the eastern Flemish Pass, warmer high salinity North Atlantic Current water flows northward contributing to a topographically induced anticyclonic gyre over the central portion of the Cap.

Satellite altimetry data are used over a large spatial area to calculate the annual-mean anomalies of the Labrador Current transport (Han et al. 2014). A total of nine cross-slope satellite altimetry tracks are used to cover the Labrador and northeast Newfoundland Slopes from approximately 47°N to 58°N latitude (Figure 41). Similarly, five tracks from approximately 55°W to 65°W longitude are used for the Scotian Slope. The nominal cross-slope depth ranges used for calculating the transport are from 200 to 3,000 m isobaths over the Labrador and northeast Newfoundland Slopes and from 200 to 2,000 m isobaths over the Scotian Slope, with the nominal depth range from 0 m to 500 m for the former and from 0 m to 100 m for the latter.

An empirical orthogonal function (EOF) analysis of the annual-mean Labrador Current transport anomalies was carried out. An index was developed from the time series of the first EOF mode and normalized by dividing the time series by its standard deviation. The mean transport values are provided based on ocean circulation model output over the Labrador and northeast Newfoundland Slopes (Han et al. 2008) and over the Scotian Slope (Han et al.1997). The mean transport along the Labrador and NE Newfoundland Slope is 13 Sv with a standard deviation of 1.4 Sv, and on the Scotian Slope it is 0.6 Sv with a standard deviation of 0.3 Sv. The mean transport values will be updated as new model output becomes available. The standard deviation values will be updated as knowledge on nominal depth improves.

The annual-mean Labrador Current transport index shows that the Labrador Current transport over the Labrador and northeast Newfoundland Slope was out of phase with that over the

Scotian Slope for most of the years over 1993-2018 (Figure 42). The transport was strongest in the early 1990s and weakest in the mid-2000s over the Labrador and northeast Newfoundland Slope, and weakest during those time periods over the Scotian Slope. The Labrador Current transport index and the winter NAO index were positively and negatively correlated over the Labrador and northeast Newfoundland Slopes and over the Scotian Slope respectively. In the past three years the annual-mean transport of the Labrador Current was above normal by about 1 SD over the Labrador and northeast Newfoundland Slopes (+1.2, +1.0 and +1.7, respectively for 2016, 2017 and 2018) while on the Scotian Shelf the transport has been below normal for the past five years (ranging between -0.7 to -1.3 SD).

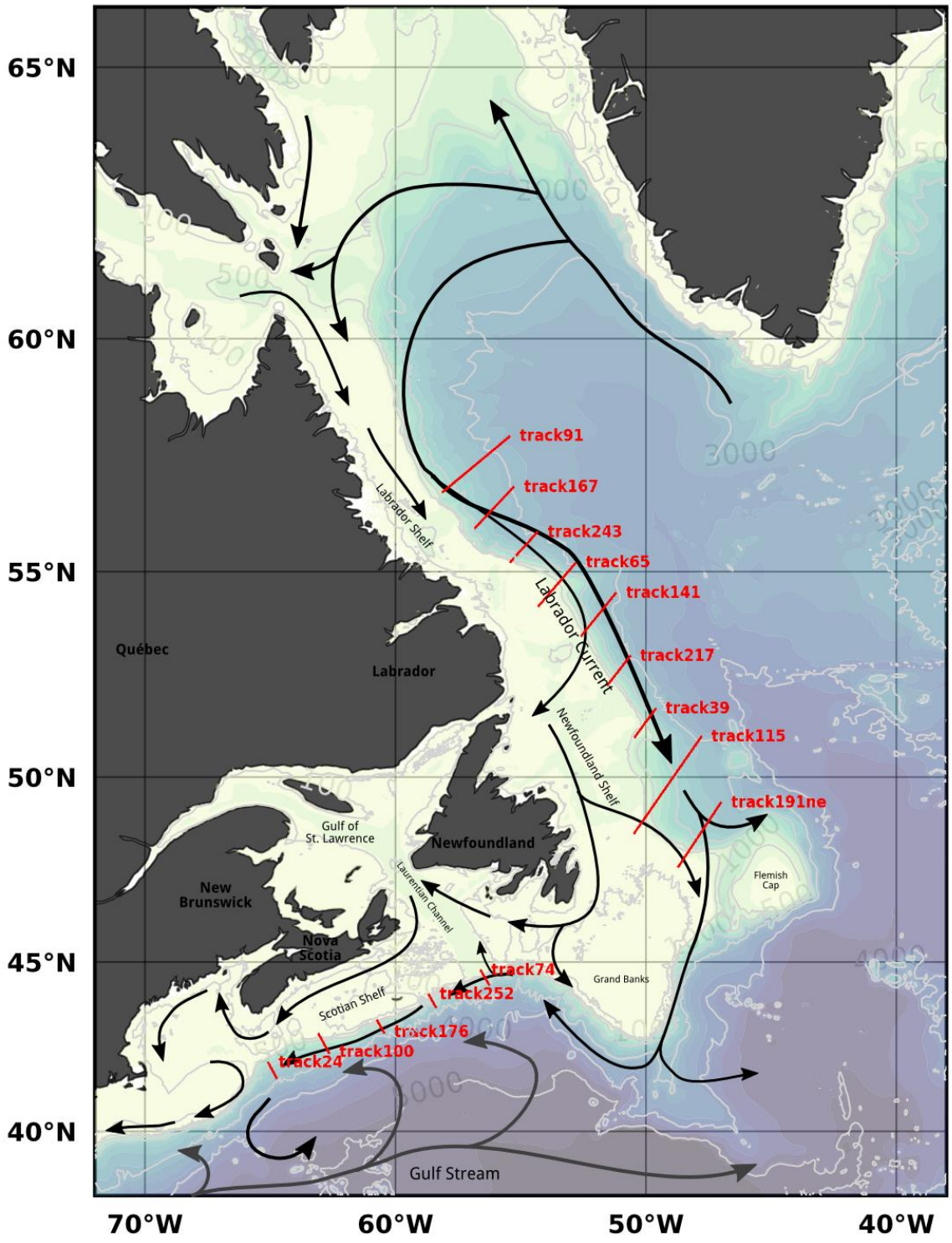

Figure 41. Map showing the Northwest Atlantic bottom topography (depth contour values in light gray) and schematic flow patterns (arrows). The Labrador Current transport is calculated across the cross-slope sections (red lines) identified by their satellite ground tracks numbers. The series of northern tracks are used for the Labrador and northeast Newfoundland slope calculation, while the series of tracks in the south are used for the Scotian Shelf slope transport calculation.

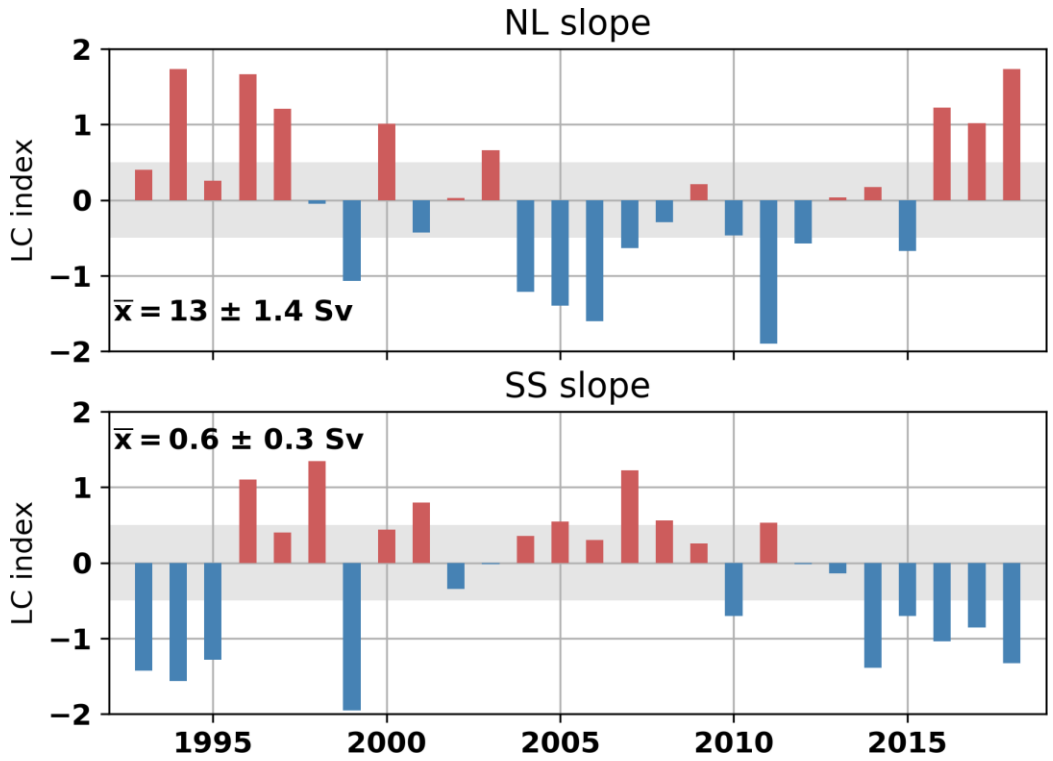

Figure 42. Normalized index of the annual-mean Labrador Current transport for the Labrador and northeast Newfoundland Slope (top) and the Scotian Slope (bottom). Long-term averages over 1993-2018 (with standard deviation) are 13 ±1.4 Sv for Labrador and northeast Newfoundland Slope and 0.6 ±0.32 Sv for the Scotian Slope. Shaded gray areas represent the ±0.5 SD range considered "normal".

SUMMARY

A summary of selected time series introduced throughout this report is presented in Figure 43 as a new NL climate index between 1950 and 2018. This index, presented here under the form of a stacked bar plot of 10 equally weighted time series (NAO, air temperature, sea ice, icebergs, SST, Station 27 temperature, Station 27 salinity, Station 27 CIL, CIL volume along hydrographic sections and NL bottom temperature), can be interpreted as a measure of the overall state of the climate system with positive values representing warm-salty conditions with less sea-ice and conversely negative values representing cold-fresh conditions. It replaces the Composite Environmental Index (CEI) from Petrie et al. (2007) presented in similar reports on NL physical conditions until now (e.g., Cyr et al 2019).

Figure 43 highlights the different regimes prevailing since 1950. For example, the 1960s stands out as the warmest period in the time series while the early 1990s is the coldest. The warming trend from the early 1990s that peaked in 2010 was followed by recent cooling that peaked in 2015. In recent years, the time series constituting the NL climate index have been nearly evenly spread between positive and negative anomalies, with salinity being the most negative since 1970.

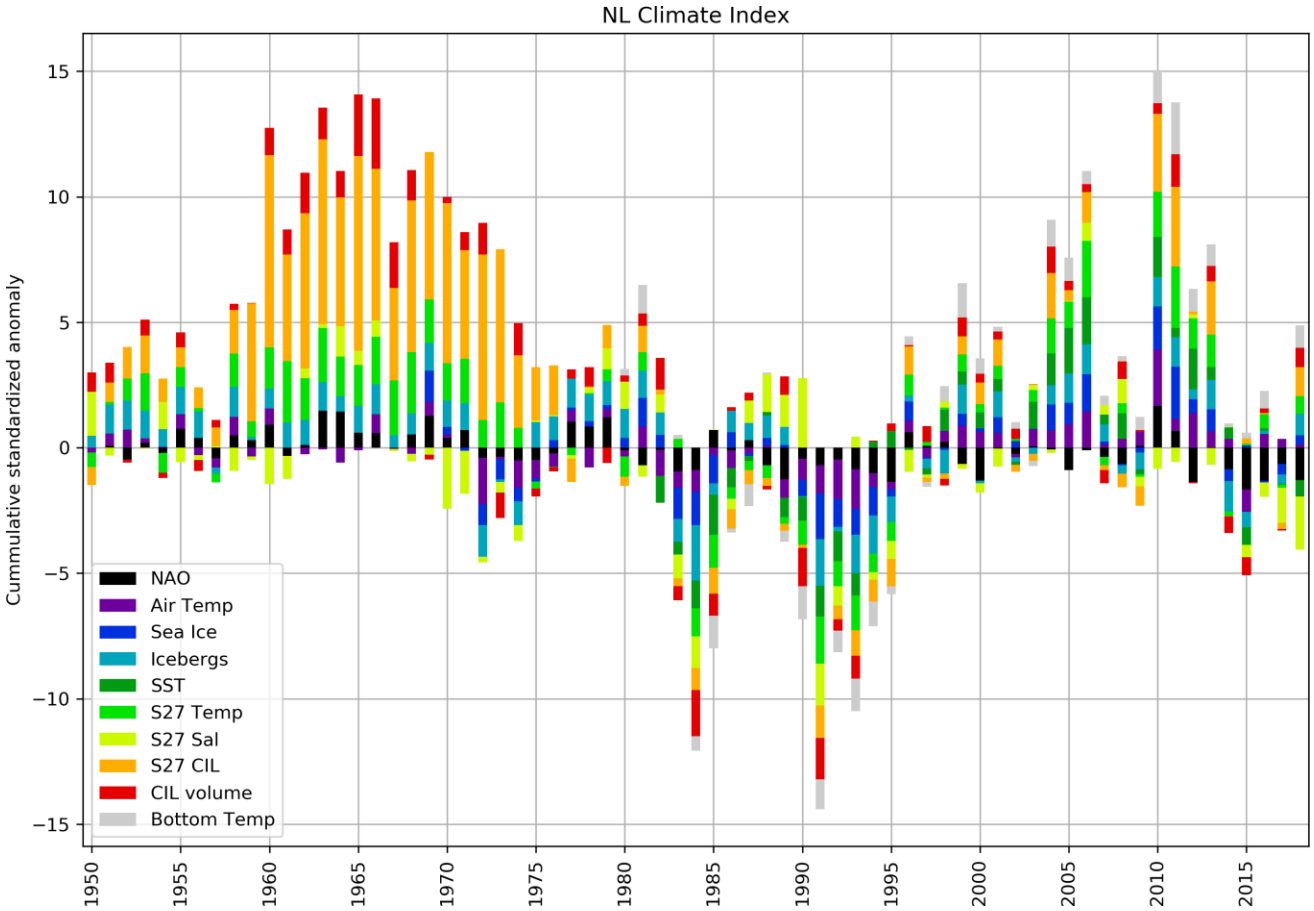

Figure 43. Newfoundland and Labrador climate index derived by summing, in a stacked bar plot, the normalized anomalies of various time series presented in this report. The time series (which start in 1950 unless specified) used for the climate index are as follows: NAO index (see Figure 3), the air temperature at 5 sites (see Figure 5), the sea ice season duration and total volume on the Labrador and Newfoundland shelves (see Figure 12; starts in 1969), the number of icebergs (see Figure 13), SSTs in 14 sub-regions (see Figure 17; starts in 1982), vertically-averaged temperature and salinity at Station 27 (see Figure 21), CIL mean temperature and core temperature at Station 27 (see Figure 22), the summer CIL volume of the areas of the hydrographic sections Seal Island, Bonavista and Flemish Cap (see Figure 32), and the spring and fall bottom temperature in NAFO divisions 3LNOPs and 2J3KLNO, respectively (see Figure 36 and Figure 39; both start in 1980).

HIGHLIGHTS OF 2018

- Winter NAO was relatively high at 1.3 SD above normal, but unusual spatial patterns in the sea level pressure over the North Atlantic have led to strong seasonal variations in air temperature (warm March over the Arctic, cold spring and warm summer at mid-latitude).
- Overall, the annual average air temperatures around the Northwest Atlantic were normal.
- Caused by the warm air temperatures in March, the sea-ice seasonal cycle exhibited a mid-season dip in ice volume, but it increased again in April to end with near-normal timing. The maximum seasonal volumes were slightly below normal on both the Labrador Shelf and the Newfoundland Shelf.
- The sea surface temperatures were mostly below normal (with some sites near normal) in the Northwest Atlantic and over the NL shelves.

- Warm anomalies were measured at Station 27, and 2018 had the largest fresh anomaly since 1970.
- Large warm bottom temperature anomalies were observed in NAFO Division 2 along the Labrador shelf. Bottom temperature was slightly warmer in most of NAFO Division 3, except for the center of the Grand Banks which was slightly colder.
- The summer cold intermediate layer was slightly warmer than normal, as were most subsurface portions of hydrographic sections Seal Island, Bonavista and Flemish Cap.
- Fresh anomalies were observed in the inshore areas of Seal Island, Bonavista and Flemish Cap hydrographic sections.
- The Labrador Current transport, as measured by satellite altimetry, was higher than normal on the Labrador and northern Newfoundland slope and weaker than normal on the Scotian slope.
- The Labrador Current transport index along the Labrador and northern Newfoundland slope was at a record high since the beginning of the time series in 1993 (equal with 1994 at +1.7 SD) while it was lower than average on the Scotian slope.
- The NL climate index was close to normal with approximately the same number of parameters above and below the long-term mean.

ACKNOWLEDGEMENTS

This work is a contribution to the scientific program of the Atlantic Zone Monitoring Program. We thank the many scientists and technicians at the Northwest Atlantic Fisheries Centre for collecting and providing much of the data contained in this analysis and to the Marine Environment Data Section of Fisheries and Oceans Canada in Ottawa for providing most of the historical data. We thank Michael Hicks of the USCG International Ice Patrol for providing monthly iceberg data for the Grand Banks. We also thank the captains and crews of the CCGS Teleost, the RV Coriolis II and CCGS Hudson for oceanographic data collection during 2018. We thank David Hebert and Nancy Soontiens for reviewing the document.

REFERENCES CITED

Casey, K.S., Brandon, T.B., Cornillon, P., and R. Evans. 2010. The past, present and future of the AVHRR Pathfinder SST Program. *In* Oceanography from space: Revisited. Edited by V. Barale, J.F.R. Gower, and L. Alberotanza. Springer, Dordrecht, The Netherlands. 273-287 p. DOI: 10.1007/978-90-481-8681-5_16.

Colbourne, E.B., Narayanan, S., and S. Prinsenberg. 1994. Climatic change and environmental conditions in the Northwest Atlantic during the period 1970-1993. ICES Mar. Sci. Symp., 198:311-322.

Colbourne, E., Holden, J., Senciall, D., Bailey, W., Craig, J. and S. Snook. 2015. Physical Oceanographic Conditions on the Newfoundland and Labrador Shelf during 2014. DFO Can. Sci. Advis. Sec. Res. Doc. 2015/053. v+ 37 p.

Colbourne, E., Holden, J., Snook, S., Han, G., Lewis, S., Senciall, D., Bailey, W., Higdon, J., and N. Chen. 2017. Physical oceanographic conditions on the Newfoundland and Labrador Shelf during 2016 – Erratum. DFO Can. Sci. Advis. Sec. Res. Doc. 2017/079. v + 50 p.

Craig, J.D.C., and E.B. Colbourne. 2002. Trends in stratification on the inner Newfoundland Shelf. DFO Can. Sci. Advis. Sec. Res. Doc. 2002/071.

Cyr, F., Colbourne, E., Holden, J., Snook, S., Han, G., Chen, N., Bailey, W., Higdon, J., Lewis, S., Pye, B. and D. Senciall. 2019. Physical oceanographic conditions on the Newfoundland and Labrador Shelf during 2017. DFO Can. Sci. Advis. Sec. Res. Doc. 2019/051.

Dickson, R.R., Meincke, J., Malmberg, S.A., and A.J. Lee. 1988. The "great salinity anomaly" in the northern North Atlantic 1968-1982. Progress in Oceanography, 20(2), pp. 103-151.

Doubleday, W.G., Editor. 1981. Manual on groundfish surveys in the Northwest Atlantic. NAFC. Sco. Coun. Studies, 2: 56p.

Drinkwater, K.F. 1996. Climate and oceanographic variability in the Northwest Atlantic during the 1980s and early-1990s. J. Northw. Atl. Fish. Sci., 18: 77-97.

Galbraith, P.S., Chassé, J., Caverhill, C., Nicot, P., Gilbert, D., Lefaivre, D. and C. Lafleur. 2019. Physical Oceanographic Conditions in the Gulf of St. Lawrence during 2018. DFO Can. Sci. Advis. Sec. Res. Doc. 2019/046. iv + 79 p.

Han, G., Chen, N., and Z. Ma. 2014. Is there a north-south phase shift in the surface Labrador Current transport on the interannual-to-decadal scale? Geophys. Res. 119: 276-287.

Han, G., Lu, Z., Wang, Z., Helbig, J., Chen, N., and B. deYoung. 2008. Seasonal variability of the Labrador Current and shelf circulation off Newfoundland. Geophys. Res. 113.

Han, G., Hannah, C.G., Smith, P.C., and J.W. Loder. 1997. Seasonal variation of the three-dimensional circulation over the Scotian Shelf. Geophys. Res. 102:1011-1025.

Hebert, D., Pettipas, R., and B. Petrie. 2012. Meteorological, Sea Ice and Physical Oceanographic Conditions on the Scotian Shelf and in the Gulf of Maine during 2011. DFO Can. Sci. Advis. Sec. Res. Doc. 2012/055. iv + 42 p.

International Commission for the Northwest Atlantic Fisheries. 1978. List of ICNAF standard oceanographic sections and stations. ICNAF selected papers #3.

Kerr, R.A. 2000. A North Atlantic Climate Pacemaker for the Centuries. Science 288 (5473), 1984-1985.

Petrie, B., Pettipas, R.G., and W.M. Petrie. 2007. An overview of meteorological, sea ice and sea surface temperature conditions off eastern Canada during 2006. DFO Can. Sci. Advis. Sec. Res. Doc. 2007/022.

Petrie, B., Akenhead, S., Lazier, J., and J. Loder. 1988. The cold intermediate layer on the Labrador and Northeast Newfoundland Shelves, 1978-1986. NAFO Sci. Coun. Studies 12: 5769.

Therriault, J.-C., Petrie, B., Pepin, P., Gagnon, J., Gregory, D., Helbig, J., Herman, A., Lefaivre, D., Mitchell, M., Pelchat, B., Runge, J., and D. Sameoto. 1998. Proposal for a northwest Atlantic zonal monitoring program. Can. Tech. Rep. Hydrogr. Ocean Sci. 194: vii+57 pp.

Thyng, K.M., Greene, C.A., Hetland, R.D., Zimmerle, H.M., and S.F. DiMarco. 2016. True colors of oceanography: Guidelines for effective and accurate colormap selection. Oceanography 29(3):9-13.

Vincent, L.A., Wang, XL., Milewska, E.J. Wan, H., Yang, F., and V. Swail. 2012. A second generation of homogenized Canadian monthly surface air temperature for climate trend analysis. Geophys. Res. 117.